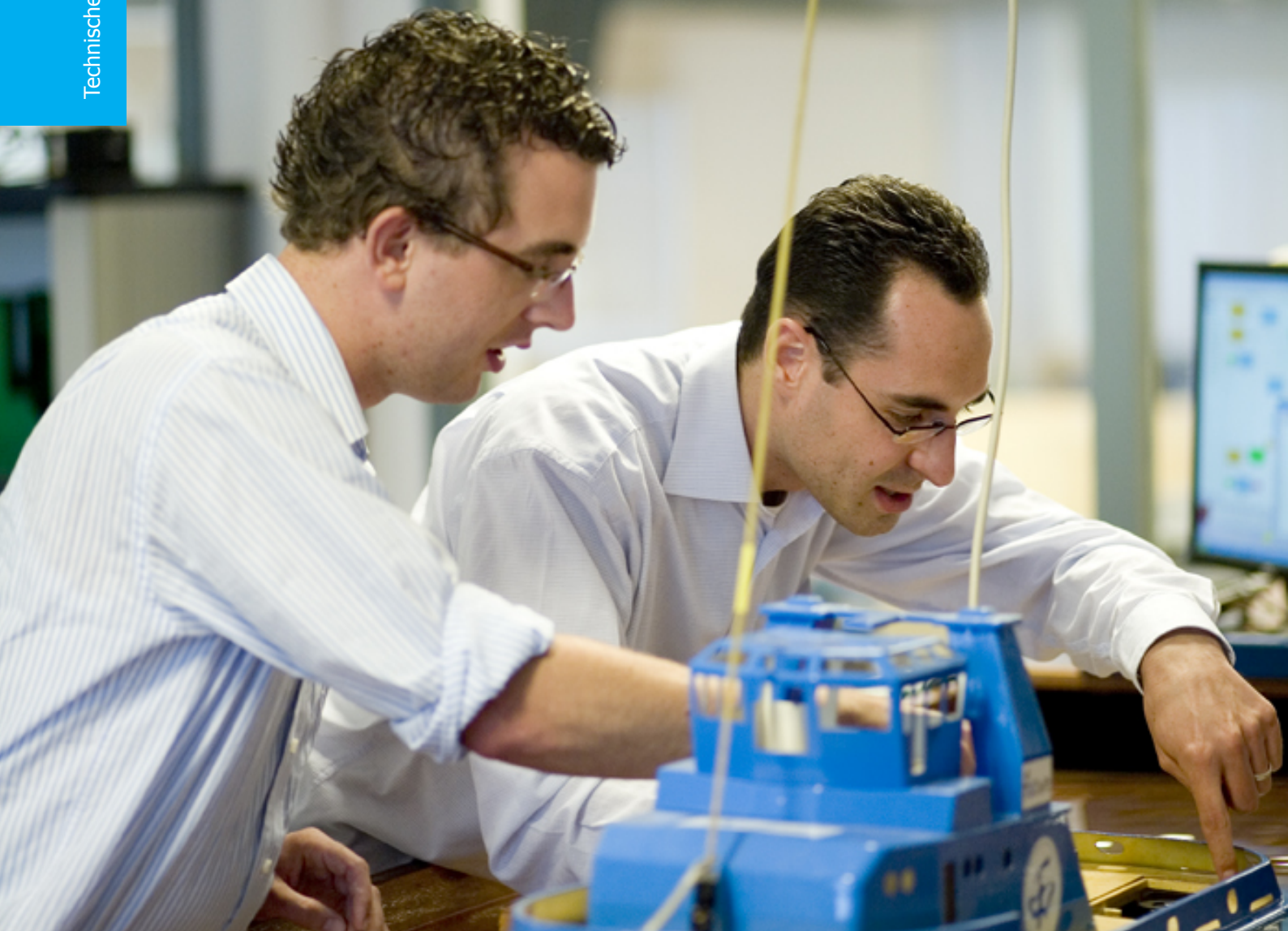


China Digital Radio (CDR) Receiver Design and Development with FM Interference Cancellation

Yiling Zhang

Technische Universiteit Delft



China Digital Radio (CDR) Receiver Design and Development with FM Interference Cancellation

by

Yiling Zhang

in partial fulfillment of the requirements for the degree of

Master of Science
in Electrical Engineering

at the Delft University of Technology,
to be defended on Monday July 4, 2016.

Supervisor:	Dr. Hong Li,	NXP Semiconductors
	Dr. ir. Gerard Janssen,	TU Delft
Thesis committee:	Dr. O. A. Krasnov,	TU Delft
	Dr. Nur Ergin,	NXP Semiconductors

This project is funded by NXP Semiconductors and executed in NXP CRD in Eindhoven, The Netherlands.

An electronic version of this thesis is available at <http://repository.tudelft.nl/>.

Abstract

A Chinese Digital Radio (CDR), labelled as GY/T 268-2013 [1], has been made and become effective in 2013 by SGAPPRFT (State General Administration of Press, Publication, Radio, Film and Television), which is an In-Band On-Channel (IBOC) digital audio broadcasting hybridized with analog FM signal in one FM channel. This report investigates the interferences to the CDR digital signals caused by both co-channel and adjacent-channel FM signals, and proposes solutions to combat such influences.

Besides an introduction on the CDR and FM broadcasting standard, a literature investigation and a theoretical analysis has been given concerning the FM interference to the CDR digital signal and existing solutions [2]. A new acquisition algorithm is implemented to realize mode detection and synchronization for the hybrid signal. Two FM interference removal methods have been proposed and studied in simulation. An energy detector is introduced to select the best FM interference removal method in run time. The different CDR modes have been added to one existing CDR simulation chain. And the receiver performance in each mode has been studied in the AWGN and TU6 multipath channel conditions. The complete simulation chain will be used for future product development.

The proposed solution has reached very good reception performance against co-channel FM interference in commonly used CDR modes. For the adjacent-channel FM interference, if we can detect and select the better removal method in real time, the performance degradation can be controlled to a limited SNR increase under the AWGN channel.

Preface

I would like to thank Dr. Hong Li from NXP Semiconductors for giving me numerous helpful instructions on both the approaches to scientific researches and the project itself, and supporting me during the whole project;

I would like to thank Dr.Ir Gerard M. Janssen from Delft University of Technology for supporting me during the project, giving me useful comments and instructions on both the project and the report;

I would like to thank Dr. Nur Ergin from NXP Semiconductors for providing me with new ideas and suggestions on the research;

I would like to thank Dr. O.A. Krasnov from Delft University of Technology for giving great lectures which help me in this project to have a better understanding on the propagation properties of radio waves and the principles behind a radar system;

I would like to thank Prof.Dr.Ir Alle-Jan Van der Veen from Delft University of Technology for the support and encouragement in this project;

I would like to thank my colleagues in NXP, Audrey Cuenin, Magda Ursulean and Wendy Zhang for accompanying and encouraging me during this project;

I would like to thank my parents for their support on both my life and study.

Yiling Zhang
Eindhoven, June 2016

Contents

1	Introduction	1
1.1	Project Background	1
1.2	Existing Digital Radio Techniques	1
1.2.1	New-band Approach	1
1.2.2	IBAC (In-Band Adjacent-Channel) Approach	2
1.2.3	IBOC (In-Band On-Channel) Approach	2
1.3	Problem descriptions.	4
1.4	Project goals.	4
1.5	Project overview.	4
1.6	Report Structure	5
2	CDR Standard and FM Broadcasting Introduction	6
2.1	CDR Standard Introduction	6
2.1.1	Spectrum Modes	6
2.1.2	CDR Transmitter Diagram	7
2.1.3	Frame Structure	8
2.1.4	Transmission Modes	10
2.1.5	Comparison with HD Radio.	10
2.2	FM Broadcasting	10
2.3	Network planning for FM broadcasting	12
3	Literature overview and theoretical analysis	14
3.1	Literature overview.	14
3.1.1	The compatibility of the hybrid system	14
3.1.2	FM interference cancellation from the transmitter side	14
3.1.3	FM interference cancellation from the receiver side	15
3.2	Theoretical analysis	15
3.2.1	Co-channel FM interference	15
3.2.2	Adjacent-channel FM interference.	18
4	Architecture design	21
4.1	Transmitter chain model	21
4.2	Receiver architecture design	22
4.3	Settings and demo	24
5	Mode detection and synchronization	26
5.1	Robustness mode detection.	26
5.1.1	Proposed algorithm.	27

5.2	Spectrum mode detection	29
5.2.1	Proposed algorithm.	30
5.3	Carrier frequency offset correction	32
5.3.1	Proposed algorithm.	32
6	Adjacent-channel FM signal interference removal	34
6.1	Energy Detector.	35
6.2	FM interference removal.	36
6.2.1	Frequency-domain (FD) method	36
6.2.2	Time-domain (TD) method	37
7	Simulation results and performance analysis	40
7.1	Acquisition performance	40
7.2	The impact of co-channel FM on the reception performance	41
7.3	The impact of adjacent-channel FM on the reception performance	45
8	Conclusions and recommendations	51
8.1	Conclusions	51
8.2	Recommendations for future work	51
A	Electric field Calculation	53
A.1	Service field strength.	53
A.1.1	P_e	53
A.1.2	$E_1(50, 50)$	54
A.1.3	G_r	56
A.1.4	Correction factor	56
A.2	Interference field strength.	57
A.2.1	$E_1(50, T)$	57
A.3	Coverage area of a station.	58
A.4	An example	58
B	Demo instructions	62
B.1	Instructions	62
B.2	Configurations	63
B.3	Saving I/Q data.	64
B.4	History	65
B.5	Operating mode.	65
C	A list of abbreviations	67
	Bibliography	69

1

Introduction

1.1. Project Background

Several digital audio broadcasting standards have been developed worldwide in recent years. The advantages over their traditional analog counterparts include higher audio quality (CD quality), higher frequency utilisation, and providing data services in addition to the audio content (e.g. traffic, weather, finance information). Thus, digitisation becomes a main tendency in the development of broadcasting systems.

A Chinese Digital Radio (CDR), labelled as GY/T 268-2013 [1], has been made and become effective in 2013 by SGAPPRFT (State General Administration of Press, Publication, Radio, Film and Television), which is an In-Band On-Channel (IBOC) digital audio broadcasting hybridized with analog FM in one FM channel. It is similar to the HD-Radio in the USA, but more suitable for China's existing FM broadcasting system. At present, several CDR test networks have been launched in Beijing, Guangzhou and Shenzhen [3]. Further large-scale implementation is also on the agenda. Therefore, to design a high-quality digital receiver is demanding and necessary for NXP to have a share in the Chinese market.

1.2. Existing Digital Radio Techniques

Three approaches are available worldwide to realize digital radio broadcasting, which are categorized by whether the digital transmission is inserted to a new band, in an adjacent FM (or AM) channel or in an FM (or AM) channel.

1.2.1. New-band Approach

The new-band approach uses new spectrum separated from the existing broadcasting band for digital transmission. One typical example is the Eureka-147 DAB System, which was developed in Europe and became a world-wide standard in 1994 [4]. It operates in L-Band (1452-1492 MHz) and Band III (174-240 MHz).

One broadcaster may use a single radio signal (called ensemble) to transmit numerous channels. The overall bandwidth is about 1.536 MHz, providing a useful capacity of 1.5 Mbit/s for a complete en-

semble. By allocating different bit rates to each channel, the number of channels to be transmitted can be flexible. Usually, the audio bit rate ranges from 8 kbit/s to 384 kbit/s, which allows the transmission of 5 to 6 high-quality stereo radio programs or 20 restricted-quality mono programs. A lower average bit rate results in a larger number of channels with a lower audio quality. However, the biggest issue of Eureka-147 is its requirement for a new spectrum band allocation.

1.2.2. IBAC (In-Band Adjacent-Channel) Approach

The IBAC approach uses an adjacent FM or AM channel to transmit the digital signal. DRM (Digital Radio Mondiale) is one of the standards using such approach. Endorsed by the ITU in 2002 [5], DRM aims to facilitate the conversion from analog to digital services for the bands below 30 MHz. Therefore, it is also called 'digital AM' or DRM30. In order to realize simulcast with analog AM signals, the bandwidth of DRM30 is constrained to 4.5 kHz or 5 kHz (half of the channel bandwidth for radio broadcasting below 30 MHz). In a new version of the specification, the bandwidth is defined to be either 10 kHz or 20 kHz (by combining two adjacent channels), in order to achieve a higher bit rate of 34.8 kbit/s or 72 kbit/s respectively.

In 2009, an extended version of DRM (called DRM plus) was ratified to allow its operation in the VHF band. Its occupied bandwidth is 100 kHz, with audio bit rates ranging from 35 kbit/s to 185 kbit/s where the required SNR (signal-to-noise ratio) is from 2 to 14 dB. The DRM+ signals are transmitted in an adjacent FM channel band, and up to four programs are available on one carrier frequency. Figure 1.1 gives an example of the configuration for DRM+ with an FM analog signal being present. As we can see, the DRM+ signal can be put to the left or right of the FM signal under robustness mode E. A minimum carrier frequency spacing $\Delta f = 150\text{kHz}$ and a corresponding power difference $\Delta p \geq 20\text{dB}$ are suggested in the standard [6].

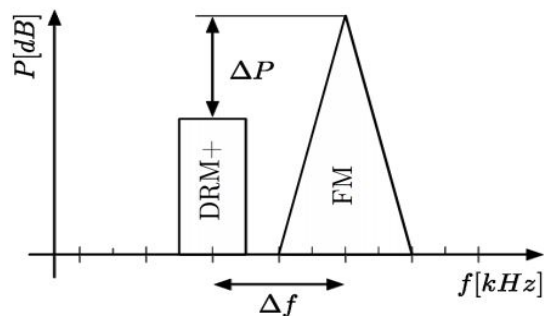


Figure 1.1: Configuration for DRM+ and FM signal

1.2.3. IBOC (In-Band On-Channel) Approach

The IBOC approach refers to the spectral placement of digital signals in occupied channels of the existing analog signals. Compared with the previous two approaches, there is no need for additional spectrum allocation. The most popular product using the IBOC approach is the HD radio in the USA. Here we will emphasize on the HD FM radio although the HD AM radio is also available in the market.

In the USA, the bandwidth of one FM channel is 200kHz and separation between two adjacent channels is also 200kHz. There are three spectrum modes in HD FM Radio, as shown in Figure 1.2, [7].

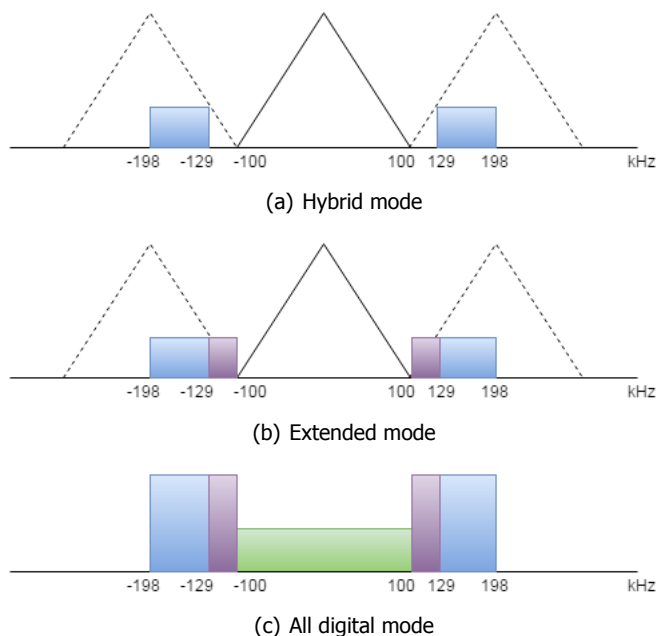


Figure 1.2: Spectrum modes for HD Radio

Figure 1.2(a) is the hybrid mode where the 70 kHz *Primary Main sidebands* are added to both sides of the host FM signal. In Figure 1.2(b), *Primary Extended sidebands* are added between host FM and *Primary Main sidebands*, making full use of the spectrum. Figure 1.2(c) is the realization of all digital transmission, where the host FM is replaced by *Secondary sidebands* with a lower power level and the *Primary sidebands* remain the same as before. As depicted in Figure 1.3, the lower-level *Secondary sidebands* help to interlace *Primary sidebands* on adjacent stations and allow the digital signals from the adjacent channel to propagate further with less interference. The maximum data rate provided by HD Radio is 277 kbit/s, with audio rate of 96 kbps plus 181 kbps rate for supplementary data or 64 kbps for audio and 213 kbps for supplementary data [8].

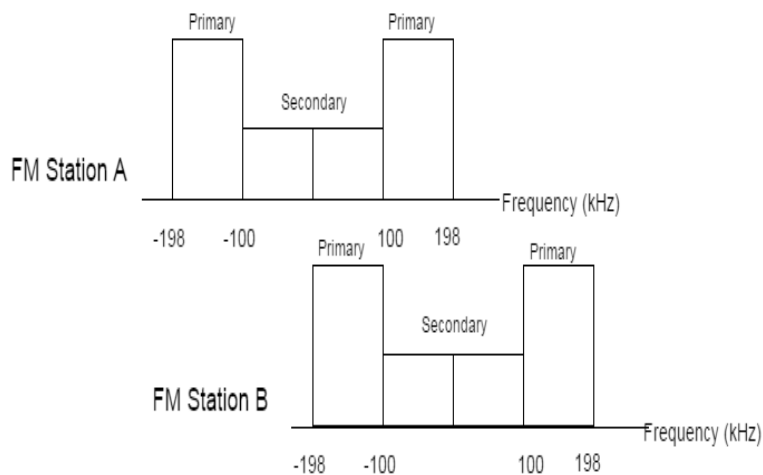


Figure 1.3: All digital mode for two FM stations

1.3. Problem descriptions

My research interest in such an IBOC system defined by the CDR standard is to investigate the mutual interference between the traditional FM signal and the newly added digital signal and to improve the digital receiver's performance in the presence of both co-channel FM signal and adjacent-channel FM signal interference.

For co-channel FM interference, one investigation is to clarify the SIR (signal-to-interference ratio) of the overlapped digital signal to the FM signal in the digital sidebands and what degradations it will cause to the digital receiver's performance (e.g. bit error rate).

As for the adjacent channel interference, questions that need to be answered are how serious the impact of the adjacent-channel FM signal would be on the host digital signal in different settings following the network-planning in China, how to detect the existence of this interference and how to eliminate its influence.

Moreover, for an existing receiver solution [2], the receiver performance degradation due to the FM interference needs to be investigated and solutions need to be found .

How the FM reception quality by conventional analog receivers is affected by the digital signal is also an issue. However, this influence is not significant and not a focus in this project due to effort limitation.

1.4. Project goals

The goals of the project include:

1. Investigate and report reception issues and methodologies in literature for receivers of similar IBOC and IBAC radio standards or technologies , e.g. HD-Radio and DRM for FM interference;
2. Investigate FM analog interference and find solutions to optimize both outer and inner receivers;
3. Complete the existing Matlab transmitter chain for all configurations based on the standard, as well as adding service description and system information and FM interference;

1.5. Project overview

In the 8-month project, theoretical analyses and solutions are made to the existing digital receiver algorithm chain for better synchronization performance and better robustness against both co-channel and adjacent-channel FM interference. In the mean time, a demo is built with a graphical user interface to demonstrate the whole design and generate test vectors for product design and testing. My work could be concluded as the following five categorizes in Table 1.1.

Table 1.1: Project overview

Standard & literature study	Chinese FM and CDR standard study
	Literature overview on design issues on IBOC radio and OFDM-based cognitive radio
	Study the existing Matlab simulation chain
Problem definition & solutions analysis	Proposing and analyzing possible issues that may be encountered in the project
	Finding solutions to realize synchronization and mode detection for the inner receiver in the presence of co-channel FM signal
	Finding solutions to improve the decoding performance of the digital receiver in the presence of the adjacent-channel FM signal
Architecture design & implementation	Designing the architecture structure of the digital receiver
	Integrating & modifying existing Matlab transmitter chain (adding FM signal, completing the configuration for all modes)
	Verifying the understanding of the standard and the simulation chain with test vectors from the standard maker.
	Implementing the proposed algorithms
Simulations & Analysis	Building a demo with a GUI in Matlab for the whole simulation chain
	Simulating and analyzing the performance of the newly-modified digital receiver under multiple system settings
	Simulating and analyzing the performance of the newly-modified digital receiver under the influence of a co-channel FM signal
Conclusions & Documentation	Simulating and analyzing the performance of the newly-modified digital receiver under the influence of an adjacent-channel FM signal
	Drawing conclusions and making recommendations for future work
	Documenting the algorithm solutions, architecture requirements, developed chains and implementations, and testing results

1.6. Report Structure

The report is organized as follows:

Chapter 1 provides an overview on the project and research problems, together with an introduction on the existing digital radio techniques. In Chapter 2, both the CDR and FM broadcasting standard are introduced briefly. Chapter 3 gives a literature overview and a theoretical analysis concerning the problems defined in Section 1.3. The architecture design of the simulation chain, including the transmitter, the receiver and a demo, is discussed in Chapter 4. In Chapter 5, a detailed explanation of the implemented algorithms to realize mode detection and synchronization is given, and Chapter 6 explains the algorithms used for an adjacent-channel FM removal module. In Chapter 7, simulation results under different scenarios are given and in Chapter 8 conclusions and recommendations for future work are provided.

2

CDR Standard and FM Broadcasting Introduction

In this chapter, first an introduction on the CDR standard is given, followed by a comparison with HD Radio. Next, in order to investigate the FM signal's impact on the CDR performance under the hybrid mode, we study the FM broadcasting standard. Finally, the network planning for FM broadcasting in China is discussed for further investigation of the adjacent-channel FM signal interference to the CDR performance.

2.1. CDR Standard Introduction

In this section, more detailed information about the CDR standard, including a transmitter diagram, frame structures, spectrum modes and transmission modes are introduced, followed by a comparison with the HD Radio.

2.1.1. Spectrum Modes

The CDR standard provides flexible spectrum allocation schemes and allows simulcasting of the digital and the FM signals. Figure 2.1 shows six different spectrum modes available in the standard. Each block represents a bandwidth of 50kHz. Blocks in green represent digital signal sub-bands while those in gray are reserved for analog FM broadcasting. Blank blocks are unoccupied bandwidth.

Spectrum index	Spectrum block position										
	-5	-4	-3	-2	-1	1	2	3	4	5	N_f
1	DB1 (L)	DB1 (U)	DB2 (L)	DB2 (U)	DB3 (L)	DB3 (U)	DB4 (L)	DB4 (U)	DB5 (L)	DB5 (U)	1
2	0	DA1 (L)	DA1 (U)	DA2 (L)	DA2 (U)	DA3 (L)	DA3 (U)	DA4 (L)	DA4 (U)	0	2
3~8	Reserved										
9	0	DA1 (L)	DA1 (U)	DA2 (L)	DA2 (U)	DA3 (L)	DA3 (U)	DA4 (L)	DA4 (U)	0	1
10	DB1 (L)	DB1 (U)	DB2 (L)	DB2 (U)	DB3 (L)	DB3 (U)	DB4 (L)	DB4 (U)	DB5 (L)	DB5 (U)	2
11~21	Reserved										
22	DB1 (L)	DB1 (U)	DB2 (L)	DB2 (U)	DB3 (L)	DB3 (U)	DB4 (L)	DB4 (U)	DB5 (L)	DB5 (U)	1
23	0	DA1 (L)	DA1 (U)	DA2 (L)	DA2 (U)	DA3 (L)	DA3 (U)	DA4 (L)	DA4 (U)	0	2
24~64	Reserved										

Note: L represents low half subband, DB3 (L) U represents high half subband, e.g. DB3 (U)

Figure 2.1: Spectrum modes in the CDR standard

Spectrum mode 9 and 10 are hybrid modes for broadcasting a stereo FM signal and a digital signal, while the analog part in mode 22 and 23 are for broadcasting a mono FM signal. Spectrum mode 1 and 2 are defined for pure digital transmission. Figure 2.2 shows a detailed spectrum allocation scheme for spectrum mode 9 and 10.

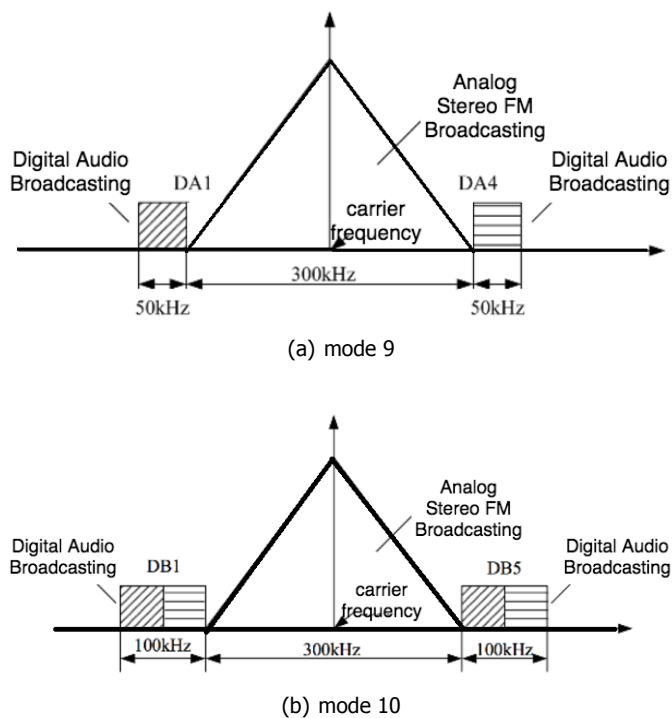


Figure 2.2: Hybrid mode spectrum (stereo FM)

2.1.2. CDR Transmitter Diagram

Three kinds of information streams can be transmitted in every CDR transmission frame, as shown in Figure 2.3, which are the MSDS (main service data symbol) that contains high-quality audio, the SDIS (service description information symbol) that carries information such as electronic program guides, and the SI (system information) that includes information as transmission modes, spectrum modes,

frame positions, constellation mapping schemes, LDPC code rates, etc. The MSDS data account for the largest proportion of the whole transmitted data, the length of the SDIS data is about 2.5% to 3% of the MSDS's length, and the SI data only contain 48 bits.

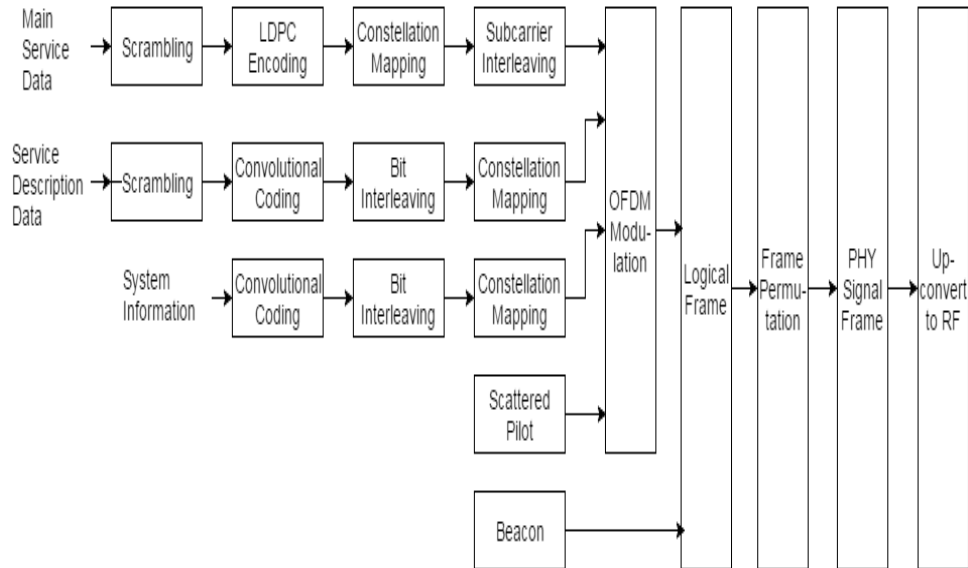


Figure 2.3: Defined CDR Transmitter Model

As depicted in Figure 2.3, these three types of data are encoded, constellation-mapped, interleaved and mapped onto OFDM subcarriers together with the scattered pilots. Considering the different lengths, there are several discrepancies when processing these three data streams. One is that LDPC codes and a subcarrier inter-leaver are used for MSDS to achieve a higher coding gain and a larger-scale interleaving gain, while convolutional codes and a bit inter-leaver are used for SDIS and SI due to their relatively short lengths. Another difference is that MSDS and SDIS data are scrambled for stronger robustness against interference and noise, and constellation-mapped via multiple schemes (QPSK, 16QAM and 64QAM) to provide various data rates. While for the SI, no scrambling is employed and only the most robust modulation scheme (QPSK) is used.

After adding the cyclic prefix and windowing functions, these OFDM modulated signals further form sub-logical frames, with a beacon signal added at the beginning of each sub-logical frame. Logical frames form physical signal frames by frame permutation (details in Section 2.1.3) and are transmitted.

2.1.3. Frame Structure

The frame structure is defined to broadcast multiple types of MSDS and SDIS information simultaneously.

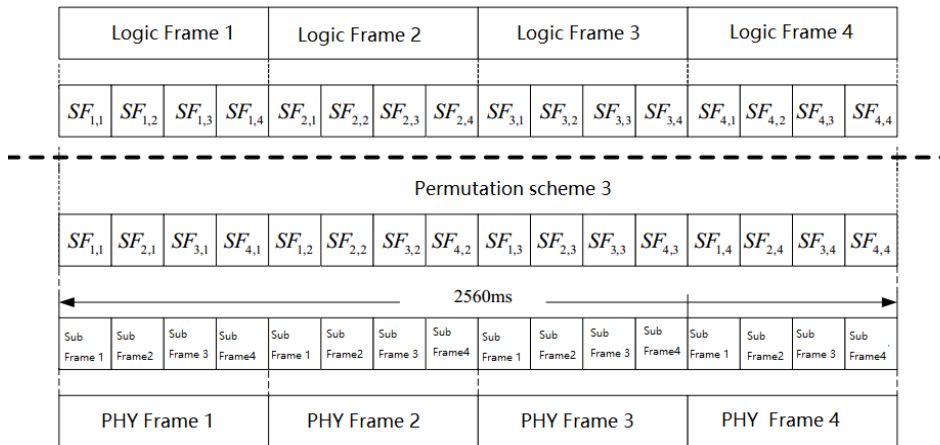


Figure 2.4: Permutation mode 3

As shown in Figure 2.4, one logic frame is composed of four logic sub-frames. The logic sub-frames in four consecutive logic frames are per-mutated according to three defined permutation modes and become a physical frame. One example is shown in Figure 2.4 of permutation mode 3. By using the permutation, multiple MSDS services can be transmitted in a more flexible way. The power consumption of the receiver devices could be saved using permutation mode 3, if the receivers need to be switched on only for one quarter of one frame’s duration. The duration of one physical frame is 640ms. Four physical frames form one superframe whose length is 2560 ms. Each sub-frame consists of one beacon and S_N OFDM symbols.

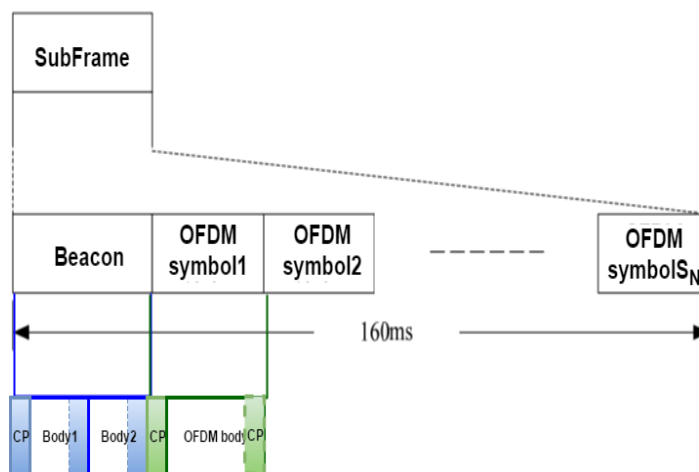


Figure 2.5: Sub-frame structure

The specially-designed structures of the beacon and OFDM symbols are important factors in designing the receiver. As shown in Figure 2.5, the body of each beacon symbol is composed of two identical parts in the time domain. Thus, the cyclic prefix is the same as the last several samples in both two parts. Each OFDM symbol is composed of an OFDM body and a cyclic prefix, which is added to combat ISI (inter-symbol interference).

2.1.4. Transmission Modes

There are three transmission modes defined in the standard, applicable for various channel environments, data rates and mobility requirements [2]. Detailed parameter settings for every mode are listed in Table 2.1, where T refers to the sample time of $1/816000$ s. Mode 1 is designed for large-scale SFN (single-frequency network) with the longest cyclic prefix which is more resistant against large delays in the SFN. Mode 2 is applicable for mobile channels because of its shorter OFDM symbol lengths and larger sub-carrier spacings. The settings of mode 3 are the same as those of mode 1 except for the shorter cyclic prefix length, and it provides a higher data rate.

Table 2.1: Specifications for different transmission modes

Parameters	Notation	Tx Mode 1	Tx Mode 2	Tx Mode 3
OFDM Body Length(ms)	T_u	2048T	1024T	2048T
OFDM CP Length(ms)	T_{cp}	240T	140T	56T
OFDM Subcarrier Spacing(Hz)	Δf	398.4375	796.8750	398.4375
Beacon CP Length(ms)	T_{Bcp}	384T	332T	168T
Beacon Body Length(ms)	T_{Bbody}	2048T	1024T	2048T
Beacon Subcarrier Spacing(Hz)	$(\Delta f)_b$	796.875	1593.75	796.875
OFDM Symbols/SubFrame	S_N	56	111	61
Valid Subcarriers	(N_v)	242	122	242

2.1.5. Comparison with HD Radio

Compared with the HD Radio, the CDR standard provides a higher bit rate, more flexible spectrum schemes, better mobile performance against Doppler effects, a higher coding gain [9] and possibilities for lower-power receivers. Table 2.2 lists some differences between the HD Radio and the CDR standard.

	HD FM Radio	CDR Standard
maximal bit rate	227kbit/s	712.8kbit/s
bandwidth	fixed 400kHz	100kHz—500kHz
FEC(forward error coding)	convolution code	LDPC code
receiver power consumption	no permutation no time-slicing	multiple permutation modes support time-slicing

Table 2.2: Comparison between HD Radio and CDRadio

2.2. FM Broadcasting

This section gives a brief introduction on the FM transmitter model and an implementation used in this project that is configured based on the parameters chosen from the standard [10].

A typical stereo FM transmitter, as illustrated in Figure 2.6(a), is composed of three blocks, namely the pre-emphasis filter, the stereo signal generator and the frequency modulator. For mono broadcasting, the stereo signal generation block is not needed and the input signal becomes a single mono channel instead of the left and right channels.

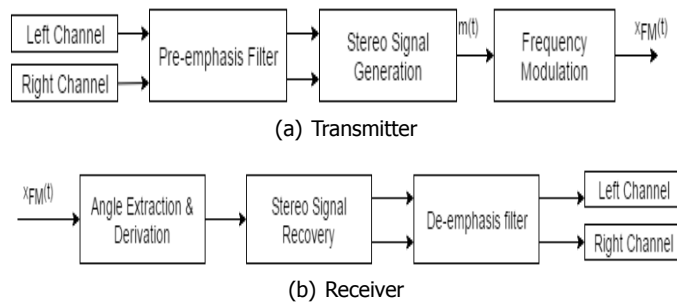


Figure 2.6: Stereo FM transceiver

The left and right channel data streams first pass the pre-emphasis filter, which amplifies the high-frequency signals. At the receiver side, a de-emphasis filter attenuates high-frequency noise and interference, resulting in a relatively high SNR for the recovered signals [11]. The frequency response of the pre-emphasis and the de-emphasis filter is $H_{pe}(f) = 1 + j2\pi f\tau_x$ and $H_{de}(f) = \frac{1}{1 + j2\pi f\tau_x}$, where τ_x is called the filter time constant.

A stereo generator is used to convert the two pre-emphasized data streams into stereophonic message signal. To comply with FM monophonic receivers, in the 30Hz-15kHz band, the signal is $L(t) + R(t)$ for monophonic reception. Stereo audio is placed in the 23-53kHz region, where $L(t) - R(t)$ is modulated onto a suppressed 38kHz sub-carrier. After adding these two signals together and passing a bandpass filter, a pilot tone is added around 19kHz which enables an FM receiver to detect and decode the stereo signal. Figure 2.7 shows the base-band spectrum of the stereo message signal and Figure 2.8 is the corresponding diagram to show how this signal is generated in Matlab for CDR simulations.

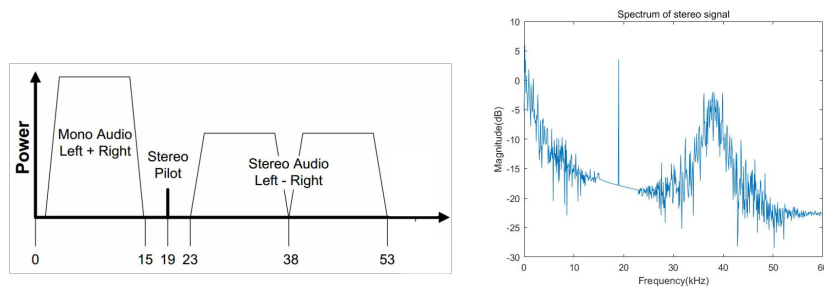


Figure 2.7: Stereo Message Signal

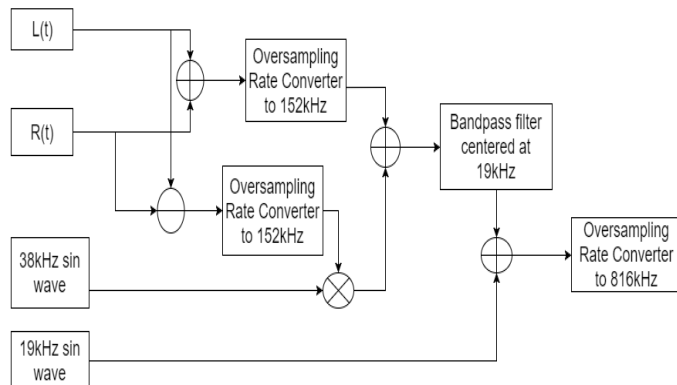


Figure 2.8: Stereo FM Generation

Finally, the FM signal is generated and expressed as the following formula:

$$x_{FM_{RF}}(t) = A_c \cos \left(2\pi f_c t + 2\pi f_d \int_{\tau=0}^t m(\tau) d\tau \right) \quad (2.1)$$

where $m(t)$ is the stereophonic message, f_d is the maximal instantaneous frequency deviation assuming the normalization condition $\max |m(t)| = 1$ and 100% modulation. A_c and f_c are the amplitude and frequency of the carrier signal.

Modulation index $\beta = \frac{f_d}{f_m}$ decides the bandwidth of the modulated signal ($BW = 2(1 + \beta)f_m$), where f_m is the maximal frequency of message signal. Table 2.3 shows the different specifications of the FM broadcasting systems used in China, the USA and Europe [12] [10]. In our simulation chain, the time constant is $50\mu s$ and the maximal frequency deviation is $\pm 75kHz$. The bandwidth for mono and stereo FM broadcasting signal is $180kHz$ and $256kHz$ respectively.

Table 2.3: Technical specifications for FM sound broadcasting at VHF worldwide

Paramters	China	USA	Europe
Broadcast band(MHz)	87-107.9	87.5-108	87.9-107.9
Channel spacing(MHz)	0.1	0.2	0.05/0.1/0.2
Time constant(μs)	50	75	50
Max. frequency deviation(kHz)	± 75	± 75	± 50

2.3. Network planning for FM broadcasting

In order to investigate the influence of an adjacent-channel FM signal on a CDR signal, which is mainly related to the power ratio of these two signals, the network planning for FM broadcasting in China is introduced in this section.

Based on the propagation model in [13] and the technical requirements specified in [14], the electric field strength of each signal can be computed at any receiver location. The field strength is related to several factors as shown in Figure 2.9.

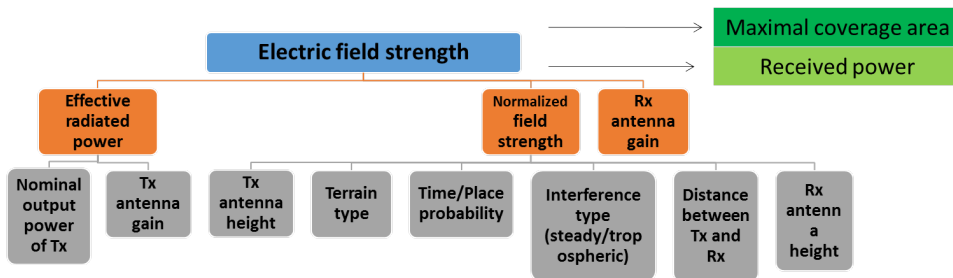


Figure 2.9: Electric field strength related factors

The coverage area of a transmission station can be determined according to the nominal usable field strength specified in [13]. Computation details are in Appendix A. Moreover, the received power may be computed as [15]:

$$P = \frac{E^2 r^2}{30} \quad (2.2)$$

where r is the distance between the transmitter and the receiver, and E is the electric field received by the user.

Furthermore, to achieve acceptable reception quality of the host station under the interference from any stations in the adjacent channels, the ratio between the field strength of the host to adjacent station is specified to exceed a certain value in the coverage range of the host station, which is defined as R.F. protection ratio in [13], as shown in Table 2.4. A more detailed discussion on the power ratio issues will be in Section 3.2.2.

Table 2.4: R.F. protection ratio

Carrier frequency spacing(kHz)	R.F. protection ratio(dB)	
	Steady interference	Tropospheric interference
0	45	37
100	33	25
200	7	7
300	-7	-7
400	20	-20

3

Literature overview and theoretical analysis

This chapter includes a literature overview and a theoretical analysis regarding the problems defined in Section 1.3.

3.1. Literature overview

Research interests on the topic of IBOC radio in literature could be divided into two categories, namely the compatibility of the hybrid system and the strategies of cancelling the FM signal from the hybrid signal.

3.1.1. The compatibility of the hybrid system

At the test stage of every IBOC standard, one important concern is: what is the compatibility of the system and how to test and define it. In [16], the performances of the FM signal such as the main audio channel performance, the SCA (subsidiary communications authorization) performance, the adjacent-channel performance and the stereo subcarrier demodulation performance, in the presence of IBOC interference are analyzed. Results show that the impact of the digital signal on the analog part is negligible as long as the power level and spectral occupancy specified are followed. In [17], several figures of merit describing the performance of the CDR system and the quality of its receiver, are proposed and tested in a laboratory environment. These figures of merit include the minimum signal level and the carrier-to-noise ratio for a receiver to reach a BER of 10^{-3} . The transmission performance and the coverage of the newly proposed CDR system are investigated in [18] which provides evidence for further popularization of the standard.

3.1.2. FM interference cancellation from the transmitter side

As for the issues on FM interference cancellation, most solutions are provided from the transmitter side. For example, in [19], Haralabos proposed an algorithm to pre-compute the response of the FM signal at the digital receiver and precancel its influence at the transmitter adaptively. Therefore, the

data rate and occupied subcarriers of the digital signal vary based on the distortion of the demodulated FM signal. In [20], the method of contiguous band insertion and control channel setting is discussed to optimize Haralabos' algorithm. In [21], Laneman proposed a novel CPPC (complementary punctured pair convolutional) inner decoding scheme, where useful bits are put in the middle subcarriers at the transmitter side together with an adaptive soft combining scheme at the receiver side to improve the receiver's robustness against multipath fading and nonuniform interference channels. Another idea is to convert the digital-analog separation problem into a co-channel FM signal separation problem. One example is shown in [22] where each OFDM symbol is transmitted twice with opposite signs consecutively. Various algorithms of co-channel FM signals separation are proposed, including a crossed-couple phase-locked loop [23], a joint Viterbi algorithm [24], an extended Kalman filtering method [25], and several combined methods [26] [27].

3.1.3. FM interference cancellation from the receiver side

From the receiver side, one practical solution available in the literature is to include multiple antennas for hybrid signals' reception [28]. A first circuit is configured and arranged to receive either the analog-type or digital-type signal by electronically steering the antennas and modifying their radiation patterns based on the estimated phase and amplitude shifts of the received signal. A second circuit combines signals received by the antennas. By using null-steering and beam-steering schemes, the interferences such as first-adjacent FM-distortions can be eliminated. However, due to the limitation of the geographical position of the transmitter and receiver antennas, there exist blank areas where no proper steering could be achieved.

Another solution is to use a CCPLL (cross-coupled phase-locked loop) [29] [23], which is composed of two PLLs that are interconnected with each other. One of the PLLs is used to lock on and track the stronger received signal while the other one tracks the weaker signal. An additional control loop is introduced to estimate the instantaneous amplitude of both received signals. However, this method is only applicable when the two received signals are both FM signals, that has the property of a constant amplitude and a modulated phase information. In the IBOC system, the hybrid signal received is a combination of a FM signal and a digital signal. The amplitude and phase of the digital signal varies all the time and cannot be locked on and tracked by a PLL.

Other concerns include how to decide whether the received signal is digital signal or FM signal in a DRM+ system. In [30], an additional reference auto-correlation block is added besides the guard-interval correlation block, to increase the detection success when the digital signal is of low power and to decrease the false alarm possibility when analog FM is received.

3.2. Theoretical analysis

3.2.1. Co-channel FM interference

The existence of the co-channel FM signal has an impact on the digital signal, which can be analyzed and dealt with both the time and frequency domain perspective.

Influence from the time domain

Looking from the time domain, the FM signal may destroy the time domain structure or correlation characteristics of both the beacon and OFDM symbols, as illustrated in Figure 2.5. Without a good correlation between the symbol body and its cyclic prefix, the receiver fails to find the start of a

subframe. One example of the impact mentioned above is shown in Figure 3.1. No obvious peak can be observed in the auto-correlation function of the hybrid signal under spectrum mode 9 and 22. Without the co-channel FM interference, an obvious peak appears in the pure digital signal case, which indicates the arrival of a subframe. Therefore, the FM signal should be filtered out sufficiently before using any time-domain processing for the digital signal, such as synchronization and mode detection.

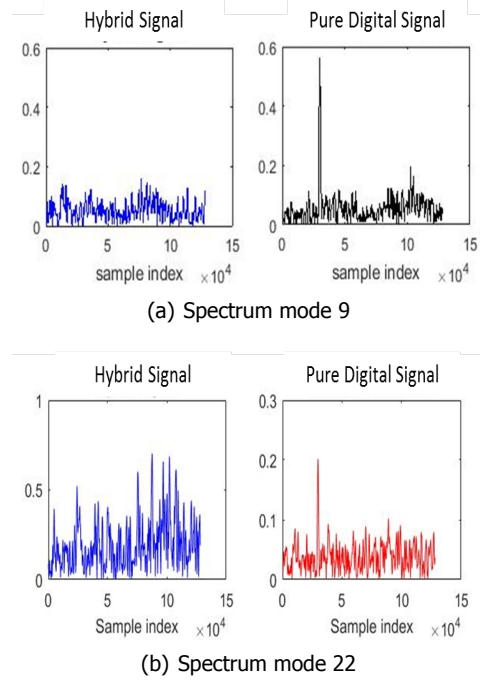


Figure 3.1: Auto-correlation function of received signal

Influence from the frequency domain

In the frequency domain, the impact of co-channel FM signal is caused by its frequency components spread in the same band as the digital signal.

The SIR value, which is defined as the power ratio of the OFDM subcarriers to the FM signal at either the upper or lower digital sideband, is an important figure of merit to analyze co-channel FM signal's impact on the digital signal. However, the power relation between the whole-band FM signal and the digital signal is often specified to hold the reception quality of the existing FM receivers. Typically, for a co-channel hybrid signal transmission, the total average power in a digital sideband should be 25 dB lower than the total power of the unmodulated analog FM carrier [31] [18] [22] [32]. Proper estimation of the SIR is yet required.

To analyze the impact of the 25 dB power ratio, both the FM signal and the digital signal are demodulated using a toolbox in Matlab. The figure of merit to analyze the influence of the added digital signal is defined as:

$$E_{FM} = \frac{1}{T} \sum (L_1(t) - L_2(t))^2 + (R_1(t) - R_2(t))^2 \quad (3.1)$$

where L_1 and L_2 are the left-channel signals demodulated from the pure FM signal and the hybrid signal respectively; $R_1(t)$ and $R_2(t)$ are the right-channel signals. By using different input audio signals in our simulations, the average value of E_{FM} is as low as -28dB, which is a negligible error. Also, we hear

no audio degradation in the received FM signal in these simulations.

The FM signal (expressed in Equation 2.1) has a constant power ($P_{FM} = \frac{A_c^2}{2}$) which is equivalent to the power of the unmodulated carrier signal. The power of the digital signal in either the upper or lower sideband is calculated as follows:

$$P_{digital} = \sum_{i=1}^{N_s} |s_i|^2 \quad (3.2)$$

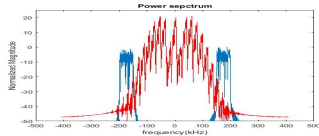
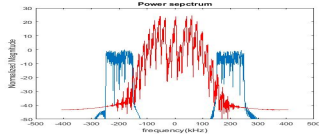
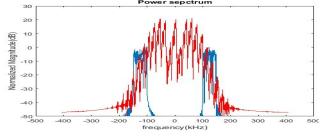
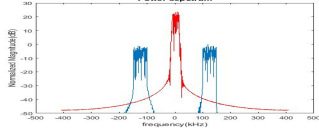
where s_i is the transmitted signal on the i_{th} subcarrier of one OFDM symbol in frequency domain and N_s is the total number of subcarriers used in either upper or lower sideband. The SIR value is computed as:

$$SIR = \frac{P_{digital}}{\sum_{i=1}^{N_s} |F_i|^2} \quad (3.3)$$

where F_i is the FM signal component on the i_{th} subcarrier of one OFDM symbol.

Table 3.1 lists several SIR scenarios with different combinations of spectrum modes and FM types. The SIR value is as high as 25dB for a combination of stereo FM signal and spectrum mode 9 or 10. When transmitting a mono FM signal and a digital signal under spectrum mode 22, the SIR value is even higher (about 40dB). However, if we combine the stereo FM signal with spectrum mode 22, the SIR ends up with a negative value (-0.5dB) which means the digital sidebands are buried under the FM signal and is impossible to be decoded.

Table 3.1: SIR in co-channel FM scenarios

FM type	Spectrum mode	Power Spectrum	SIR(dB)
Stereo	9		24.25
Stereo	10		24.916
Stereo	22		-0.5044
Mono	22		39.32

Based on the observations from Table 3.1, spectrum mode 22 and 23 are not suitable for stereo FM broadcast. It confirms that they are designed for mono broadcasting FM signals because if stereo FM signal is inserted, the SIR value will be too low to decode the digital signals. The impact of stereo (for spectrum mode 9 and 10) /mono (for spectrum mode 22 and 23) FM signal on the digital sidebands are limited even with the 25 dB power ratio.

3.2.2. Adjacent-channel FM interference

The adjacent-channel FM interference appears mainly due to a limitation on a country's network-planning scheme. When the geographical distance between two broadcasting stations that share the adjacent FM channels are not far enough, an overlap coverage zone will appear, resulting in interferences.

Similar to Section 3.2.1, the SIR value, which is defined as the power ratio of the OFDM subcarriers to the adjacent-channel FM signal at either the upper or lower digital sideband, is used to analyze the impact that the adjacent-channel FM signal causes to the digital signal. The SIR value is related to the network settings (including the carrier frequency distance and geographical distance between the two stations, and the transmit power of the stations) and the user's distance to the station.

In order to estimate the SIR value, we first decide the power ratios of the host FM to the adjacent-channel FM signals based on different network settings. With the knowledge that the power of the co-channel FM signal is 25dB higher than that of the host digital signal, the SIR value could be predicted. We assume there are two radio stations with the same transmission parameters, as shown in Figure 3.2, where station A is the host station and station B is the interfering station. The triangle represents possible positions of the digital receiver. Based on the settings in Figure 3.3, the coverage area of each station is 56 km (Computational details are in Appendix A). The distance between the station A and B is assumed as 80 km.

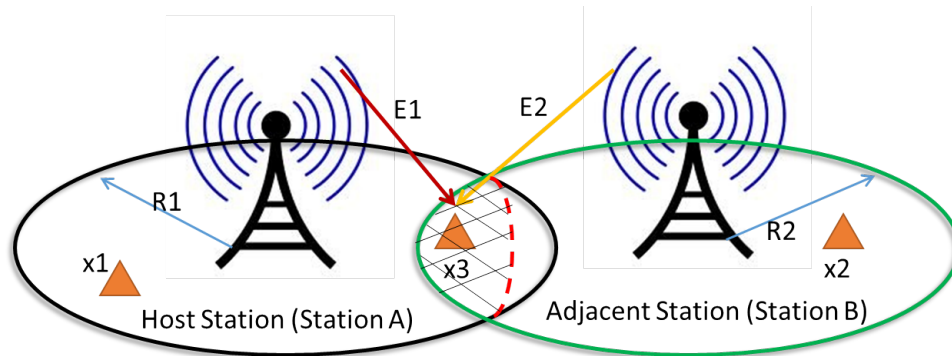


Figure 3.2: System model for the adjacent FM interference

Transmission power(dBkw)	40
Effective height of TX antenna(m)	150
Receiving antenna height(m)	2
Degree of terrain irregularity(m)	90
Path type	Urban

Figure 3.3: Transmission settings of station A and B

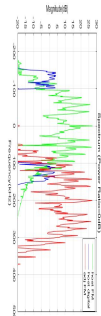
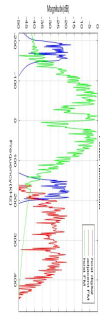
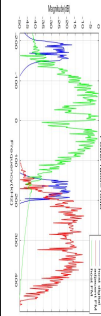
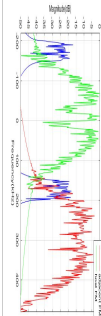
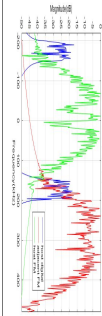
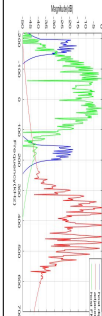
Serious adjacent-channel FM interference may happen in the slashed area such as at position x3 in Figure 3.2, where the coverage areas of station A and B overlap and the R.F. protection ratios defined in Table 2.4 is satisfied, but the received FM powers of station A and B are similar. In other cases,

when the user is at position x_1 , the signal power received from station A is much higher than that from station B, so a good reception quality is expected. By changing the carrier frequency spacing between these two stations and the user's distance from the host station, different power ratios of the host station to the interfering station can be computed (details in Appendix A). Table 3.2 list several scenarios based on the above settings, and the digital signal here is under spectrum mode 9.

When the carrier frequency spacing is 200 kHz, as shown in the first scenario in Table 3.2, there is even serious mutual impact between the host FM and the adjacent-channel FM signal. This situation need to be compulsorily avoided when making the network-planning in China. When the carrier frequency spacing is equal to or more than 400 kHz, the overlapped ratio between the digital signal and the adjacent-channel FM signal is quite low, which will not cause a great interference if bandpass filters are used.

Our research focus is therefore at the carrier frequency spacing of 300 kHz. As the user gets closer to the interfering station, the ratio of received power from station A to that from station B becomes smaller. In our example, when the receiver is 35 km away from station A, the power ratio received is 10 dB. When it goes 3 km closer to station B, the ratio drops to about 4 dB. The ratio becomes 0 dB when it is at the middle of these two stations. Our focus is to improve the performance of the digital receiver in this region.

Table 3.2: Scenarios of adjacent-channel FM interferences

Scenario	Δf (kHz)	d_A (km)	Power Ratio (dB)	Power Spectrum
1	200	40	0	
2	300	30	20	
3	300	35	10.16	
4	300	38	4.07	
5	300	40	0	
6	300	40	0	

d_A is the distance between user and station A

4

Architecture design

The architecture design includes three parts: a transmitter chain model which is used to generate hybrid signals for particular research scenarios and further product design and testing, an improved receiver chain updated from [2] which is used to perform investigations on the research problems, and a demo with a graphical user interface to demonstrate the whole design intuitively. This chapter explains these three parts and points out the modifications made compared with Yun's previous work [2].

4.1. Transmitter chain model

At the transmission side, we assume a linear combination of an FM broadcasting signal and a digital signal in time domain. As illustrated in Figure 4.1, we first generate the base-band digital signal and the FM broadcasting signal as discussed in Chapter 2. The amplitude scalar block is used to adjust the transmission power of the digital signal such that the power of the co-channel FM signal is 25dB higher than the digital signal, as mentioned in Section 3.2.1. Then the digital and FM signals are added in the time domain.

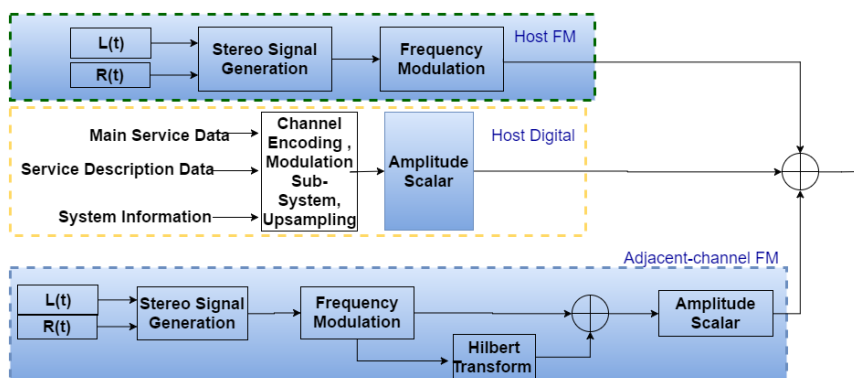


Figure 4.1: Hybrid Transmission Model

Our simulation is based on baseband signals. Therefore, instead of using the FM signal as indicated

in Equation 2.1, we use the baseband FM signal as:

$$\begin{aligned}
 x_{FM}(t) &= \text{lowpass}(x_{FM_{RF}}(t)e^{-j2\pi f_c t}) \\
 &= \text{lowpass}\left(\frac{A_c}{2}\left[e^{j2\pi f_d \int_{\tau=0}^t x(\tau)d\tau} + e^{-j(4\pi f_c t + 2\pi f_d \int_{\tau=0}^t x(\tau)d\tau)}\right]\right) \\
 &= \frac{A_c}{2}e^{j\theta(t)}
 \end{aligned} \tag{4.1}$$

with $\theta(t) = 2\pi f_d \int_{\tau=0}^t m(\tau)d\tau$. The combined hybrid signal is:

$$x(t) = x_{FM}(t) + a \cdot x_{digital}(t) \tag{4.2}$$

where a is the factor used to adjust the power of digital signal.

When the adjacent-channel FM signal is also included, the sampling rate is four times higher than before to avoid aliasing, namely 3.264 MHz. The digital signal is oversampled by padding zeros in the frequency domain when generating the OFDM subcarriers. The way to generate the adjacent-channel FM signal is the same as that of the co-channel FM signal, except that the carrier frequency is a multiple of 100kHz. After the frequency modulation block, an Hilbert transformation block is added. By adding the real-valued signal with its Hilbert transformation, the real-valued signal is transformed to a corresponding complex signal (called analytic signal) which has no negative frequency components. In this way, only the upper or lower sideband of the digital signal will be influenced by the adjacent-channel FM signal. The amplitude scalar block adjusts the power of the adjacent-channel FM signal based on its relation to the host FM signal.

Compared with Yun's simulation chain [2], the host FM and the adjacent-channel FM signal generation blocks and the amplitude scalar block are newly added. Multiple settings are implemented to be configured for all CDR digital modes, and configurable oversampling rate is realized for product test purpose.

4.2. Receiver architecture design

In this section, a design of the modified digital receiver is proposed, as shown in Figure 4.2. Implemented on a software-defined radio (SDR) platform, the design of the digital receiver is more related to software algorithm development. From the users' perspective, the digital receiver should fulfill several requirements such as a quick channel switch, acceptable audio quality and channel scanning functions. From a system design perspective, the architecture should be flexible, easy to be implemented and modified.

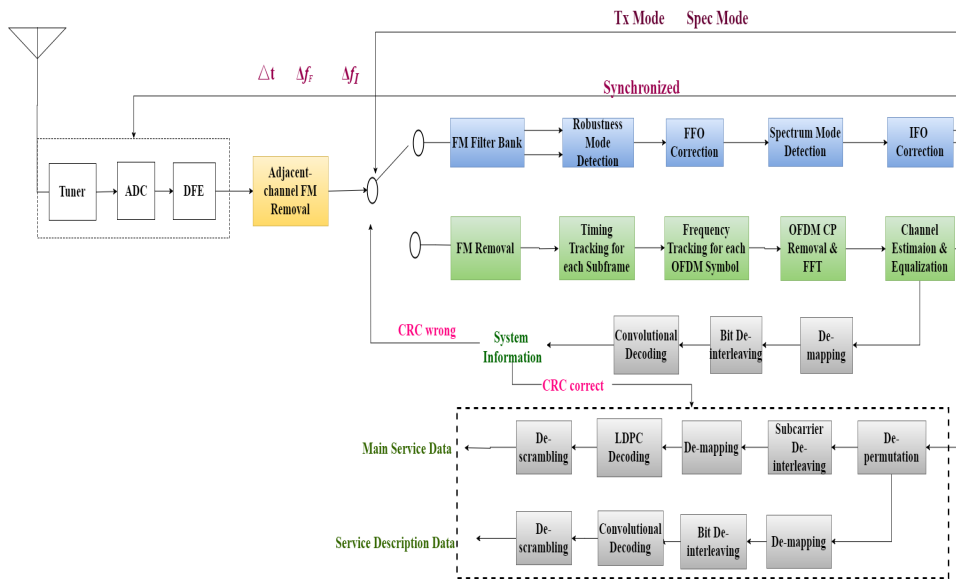


Figure 4.2: Modified Digital Receiver chain

The receiver can be divided into four functional blocks: the adjacent-channel FM interference processing block (orange blocks), the acquisition mode of the inner receiver (blue blocks), the operating mode of the inner receiver (green blocks), and the outer receiver (gray blocks).

The adjacent-channel FM removal block functions to detect the existence of adjacent-channel FM interferences and to eliminate the interference power.

The acquisition mode is operated at the beginning of each channel switch, where the transmission and spectrum mode of the received digital signal are detected, the beginning of a subframe is found under the impact of co-channel FM signal. After the co-channel FM signal is removed, the frequency offset caused by the instability of a receiver LO is compensated. The FM filter bank block filters out the signals in the possible FM sub-band, i.e. 200kHz and 300kHz, to output two parallel signal streams for further mode synchronization processing. At this stage, without any knowledge of the spectrum mode setting, the output of the FM removal block are two parallel data streams, with either 200kHz or 300kHz analog FM signals filtered out. The next block is used to estimate the transmission mode by detecting the starting position of a super-frame using correlation. When the two parallel data streams pass this block, the best correlated stream and the correlation peak position are selected as the detected mode and synchronization position. Afterwards, the fractional frequency offset of the receiver LO is detected and corrected [2]. Then we do a differential cross-correlation between the modified receiving signal and the reference beacon to estimate the spectrum mode and the arrival time of the strongest channel path. Finally, the IFO (integer frequency offset) is corrected in the frequency domain, based on the idea of a periodogram. The estimated frequency and time offset are fed back to either the tuner or the DFE (digital front-end) block to realize the frequency offset compensation..

The receiver enters its operating mode after the received signal is synchronized and its transmission and spectrum mode settings are estimated. After the FM signal is filtered out, the receiver discovers OFDM body, estimates the wireless channel to equalize the OFDM sub-carriers and demodulate them. There are also functions to track and correct the residual frequency offset of each OFDM symbol and the time offset of each sub-frame. These blocks remain unchanged compared with Yun’s previous design [2].

The outer receiver provides the user with the decoded MSDS and SDIS information. Another important function of the outer receiver is that it extracts the SI from each subframe which will be used to confirm a correct acquisition detection accuracy and obtain the overall modulation and coding settings of the digital signal. If the CRC (cyclic redundancy check) of the SI bits is wrong, the receiver will restart the acquisition mode. Otherwise, if the CRC is correct and the first subframe is found, with the permutation scheme, the constellation mapping scheme and LDPC code rate information extracted from SI, MSDS and SDIS data could be obtained from the outer receiver.

Compared with Yun's design [2], the adjacent-channel FM interference block is newly added; the acquisition mode blocks (blue blocks) are modified and improved to realize mode detection and synchronization under co-channel FM interference; the service description data are extracted from the modified outer receiver and a loop is designed to make use of the system information.

4.3. Settings and demo

Multiple modes of the CDR digital signal have been newly added in this project, including a combination of 3 transmission modes, 4 spectrum modes, 3 constellation mapping schemes and 4 LDPC code rates. One setting that is currently used in China has been tested for both the transmitter and the receiver chain using a test data set provided from SGAPPRFT. By using the test data, three types of data streams (MSDS, SDIS, and SI) have been successfully decoded, which indicates the implementation of our receiver chain is correct. Using the same settings listed in the decoded SI, our transmitter model generates the same baseband IQ samples as in the test data.

A demo has been built with a graphical user interface to demonstrate the whole design and generate test vectors for product design and testing, as shown in Figure B.1. Appendix B shows how to use the demo.

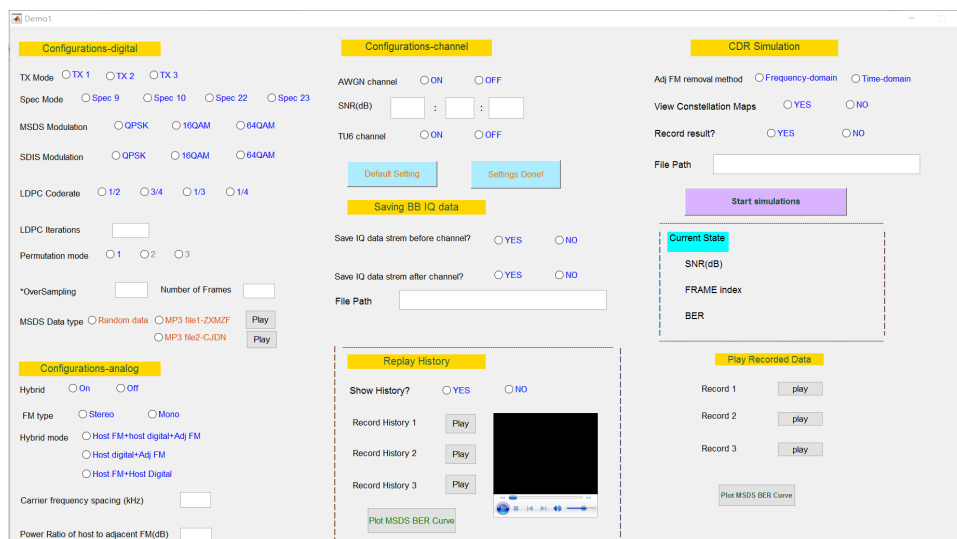


Figure 4.3: Demo

The demo realizes several functions:

- Configurable system parameters for both digital and FM signals at the transmitter side
- Configurable hybrid mode and channel environment

- Saving I/Q data streams both before and after the channel for product development test
- Showing the real-time state (in its acquisition or operation mode) and performance of the receiver (such as the constellation map of demodulated LLRs before decoding, the current frame index, the bit-error-rate, etc)
- Providing history data corresponding to the SNR values of an acceptable BER value (between 10^{-3} and 10^{-4}) based on the configurations
- Recording real-time decoded data and generating BER curves with different SNR values

5

Mode detection and synchronization

In this chapter, more detailed design of the acquisition mode blocks, namely the blocks in blue in Figure 4.2 are explained. The function of each block are introduced and the algorithms implemented are discussed and analyzed. The acquisition performance of the proposed algorithms is in Chapter 7.

The mode detection and synchronization blocks start to work at the beginning of each channel switch, which are defined as the acquisition mode of the receiver. These blocks are used to detect the start of one sub-frame (called the header detection), to correct the frequency offset, to detect the transmission and spectrum mode of the received signals under the impact of co-channel FM interference such that the receiver could work properly in its operating mode.

In Yun's design [2], for the IFO correction block, she computes the cross correlation between the power of the received signal and the reference beacon signal, which will be easily influenced by the existence of an adjacent channel interference. Therefore, modifications are made to this block in this project. Moreover, the blocks that realize the transmission and spectrum mode detection under the impact of co-channel FM interference are newly added in this project.

5.1. Robustness mode detection

The goals of robustness transmission mode detection are to detect the start of one sub-frame, to detect the transmission mode of the digital signal and to detect the bandwidth reserved for the FM signal which is defined as the first stage of spectrum mode detection in Figure 4.2.

As mentioned in Section 2.1.4 and 2.1.1, there are three transmission modes and six spectrum modes in the CDR standard which lead to 18 different combinations in total. For the different transmission modes, as shown in Table 2.1, the length of the OFDM and beacon symbols, the sub-carrier spacing, and the number of OFDM symbols per sub-frame are all different. For the different spectrum modes, the bandwidth reserved for the FM signal can be either 200kHz or 300kHz. It is important to know the length of both the beacon and the OFDM symbols such that correct parameters could be used to find the start of one subframe. Also, the bandwidth reserved for the FM signal should be determined so that either the interference brought by the FM signal is limited or no digital signals have been filtered out mistakenly.

5.1.1. Proposed algorithm

The algorithm proposed calculates the auto-correlation function by using the structure property (the repetition of the last samples as the cyclic prefix) of the digital signals and all three possible sets of parameters. It is divided into two parallel processes, which will be explained in the following section.

First-process

The first process correlates the cyclic prefix of the beacon with its body and makes use of the two identical parts in one beacon body, as shown in Figure 2.5. The auto-correlation function is computed as shown in Equation 5.1. Instead of one peak, an uncertainty plateau [33] will appear with a length of the cyclic prefix of the beacon. To eliminate this plateau, the auto-correlation is averaged over the length of the cyclic prefix, denoted as M_c in Equation 5.2.

$$\rho_2(k) = \frac{\sum_{n=1}^{N_b} r_b(n+k+N_b) \cdot r_b^*(n+k)}{\frac{1}{2} \sum_{n=1}^{N_b} (|r_b(n+k+N_b)|^2 + |r_b(n+k)|^2)} \quad (5.1)$$

$$M_c(k) = \frac{1}{L_b} \left| \sum_{n=1}^{L_b} \rho_2(k+n) \right|^2 \quad (5.2)$$

where r_b is the received signal, L_b is the length of the cyclic prefix of the beacon symbols, N is the length of OFDM symbol body, N_b is half the length of the beacon body. In RMD, we use the parameters of all three transmission modes and find the matched parameters N_b and L_b that will give a peak in M_c . The unique peak in M_c also indicates the arrival of a beacon symbol, and the sample index corresponding to the peak is the estimated starting point of a sub-frame.

Figure 5.1 shows the modified auto-correlation function $M_c(k)$ using different N_b and L_b values, when the signal is under transmission mode 2 and spectrum mode 9. The blue curves are calculated based on the residual hybrid signal after a 200kHz FM signal filter, while the red curves are those after a 300kHz FM signal filter. As we can see, only the curve with a 300kHz FM signal filter and using parameters of transmission mode 2 has an obvious peak.

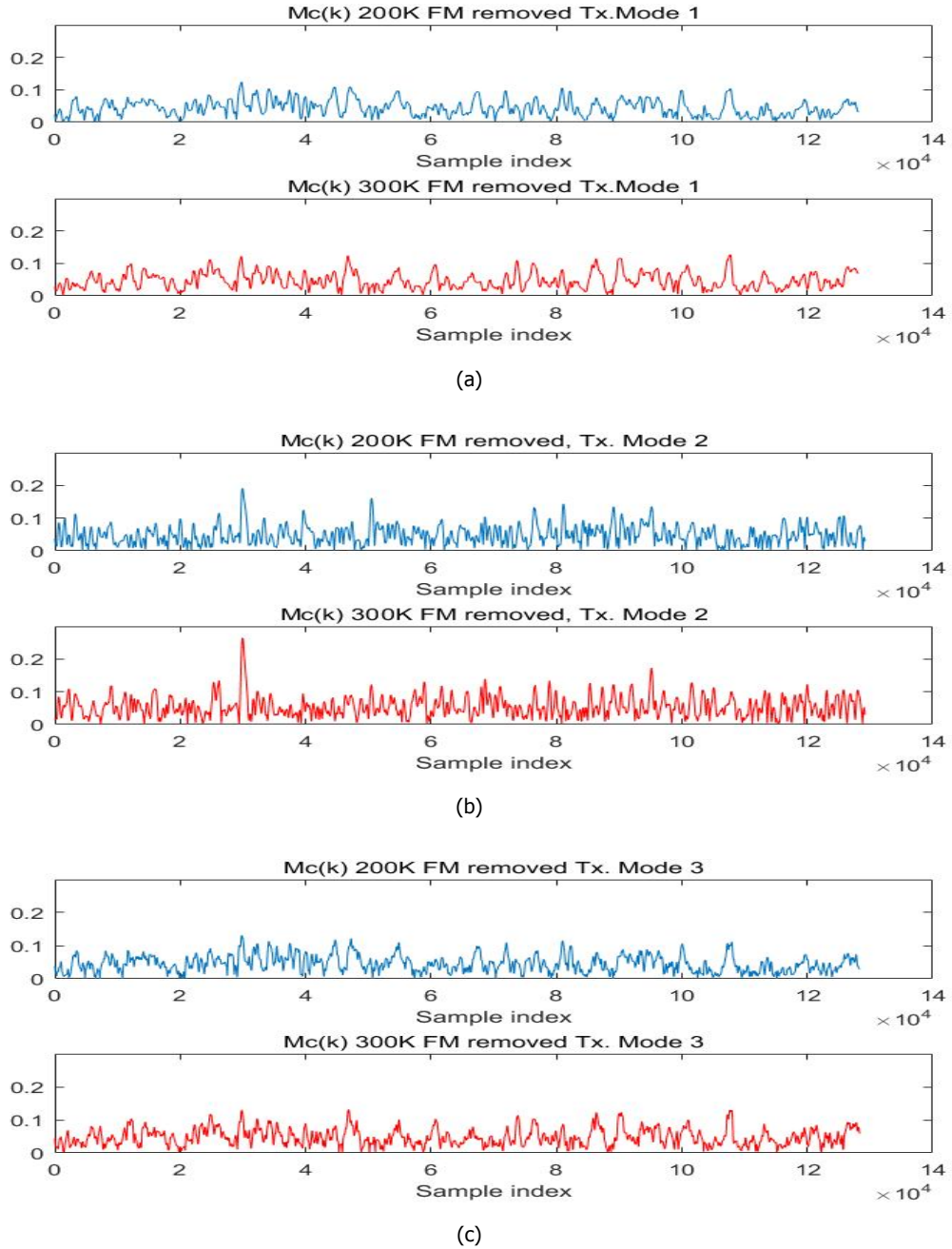


Figure 5.1: Modified auto-correlation function in RMD

Second-process

There are two reasons for why the second process is necessary. Firstly if the transmission mode is 1, M_c calculated by the parameters of transmission mode 3 also has a peak, and vice versa. This is because N_b from both modes are the same (2048). Therefore, we need a further process for RMD. Moreover, in most cases, the header of a new super-frame is in the middle of the received sequence.

The second process uses the cyclic prefix of the OFDM symbols. The auto-correlation function is defined as:

$$\rho(k) = \frac{\sum_{n=1}^L r_b(n+k+N) \cdot r_b^*(n+k)}{\frac{1}{2} \sum_{n=1}^L (|r_b(n+k+N)|^2 + |r_b(n+k)|^2)} \quad (5.3)$$

where L and N are the length of the cyclic prefix and the body of OFDM symbols respectively. Each peak indicates one OFDM symbol. Again, we traverse the three transmission modes, using the corresponding L and N to calculate three $\rho(k)$ curves. If the parameters we choose match the transmission mode of the received signal, periodic peaks will appear. Different ways of using the periodic peaks are mentioned in the literature, such as introducing a cosine function as the cost function [34], setting a threshold and using the distance between two consecutive peaks [35] or finding the global maximal value with correction factors [36].

In our project, we calculate $\rho(k)$ for N_{number} OFDM symbol durations, and add up the $\rho(k)$ s that are N_s samples apart:

$$P(k) = \frac{1}{N_{number}} \sum_{m=1}^{N_{number}} \rho(k + mN_s) \quad (5.4)$$

With the correct N and L values, there will be a cumulative high peak in $P(k)$, which will be our detected transmission mode parameters. One example is shown in Figure 5.2, with transmission mode 3 and spectrum mode 9. We can see that the peak only appears in the last subplot.

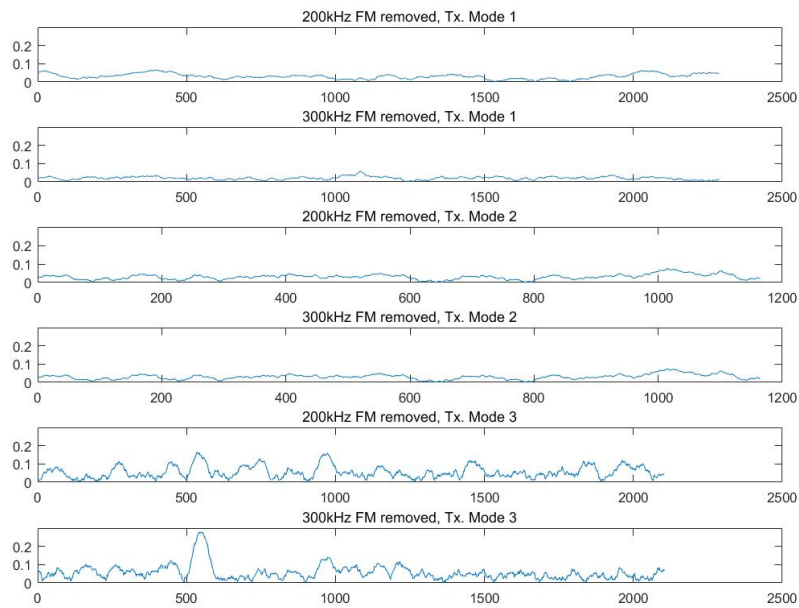


Figure 5.2: Cumulative peak method

5.2. Spectrum mode detection

The goal for this block is to determine the bandwidth of the digital signals to be either 50kHz or 100kHz, as shown in Figure 5.3. Together with the estimation of the bandwidth reserved for the FM signal from the robustness mode detection block, the spectrum mode of the received signals can be determined.

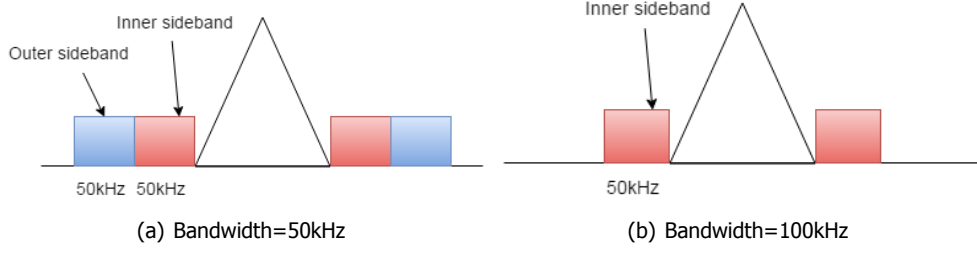


Figure 5.3: Possible spectrum modes after 1st stage detection

For different spectrum modes, the position of occupied sub-carriers for each OFDM and beacon symbol are not the same. Normally, the IFO is detected by computing the cross-correlation between the received signals and the reference beacon. Therefore, it is important to determine the spectrum mode before the IFO correction. One simple method is to convert the received beacon symbol into the frequency domain and compare the signal powers at the outer and inner sideband position. If the spectrum mode has a 100kHz bandwidth, these two values should be similar. Otherwise, the power of the outer sideband should be much smaller than the inner sideband. However, high noises, interference from adjacent channels and a deep-fading channel will all have a negative influence on the results.

5.2.1. Proposed algorithm

The algorithm we propose here computes the differential cross-correlation between the received beacon and the two known reference beacons in the time domain, and chooses the one that gives the maximal peak value as the estimated spectrum mode. In the following section, we will first explain how the differential cross-correlation method outperforms the conventional correlation scheme [37] in reducing the influence of IFO. Then the implementation of the algorithm is explained, followed by a modified version to further improve its accuracy.

The timing metric of the conventional correlation scheme is as follows:

$$\begin{aligned}
 J_1(s) &= \frac{1}{N} \sum_{n=0}^{N-1} r(n+s)S^*(n) \\
 &= \frac{1}{N} \sum_{n=0}^{N-1} \sum_{l=0}^{L_{channel}-1} c_l S(n+s-\tau_l) e^{j\frac{2\pi\varepsilon(n+s)}{N}} S^*(n)
 \end{aligned} \tag{5.5}$$

where $r(n)$ and $S(n)$ are the received beacon after FFO correction and the reference beacon signal in the time domain, respectively. N is the length of the beacon body. s is the delayed shift in sample period. $L_{channel}$ is the number of channel paths, c_l is the complex gain of the l_{th} path and τ_l is the delay of that path. $J_1(s)$ can be divided into a non-coherent part which is approximately zero and a coherent part as:

$$\begin{aligned}
 J_{1c}(s) &= e^{j\frac{2\pi s\varepsilon}{N}} c_i \frac{1}{N} \sum_{n=0}^{N-1} e^{j\frac{2\pi n\varepsilon}{N}} \\
 &= e^{j\frac{2\pi s\varepsilon}{N}} c_i \Gamma(\varepsilon)
 \end{aligned} \tag{5.6}$$

As we can see, the maximal absolute value of $J_1(s)$ depends on both the channel complex gain c_i and the factor $\Gamma(\varepsilon)$ which is related to the IFO. From Figure 5.4 we see that $|\Gamma(\varepsilon)|$ is one only when IFO is

zero. For other IFO values, $|J_1(s)|$ will become zero with the influence of $|\Gamma(\varepsilon)|$.

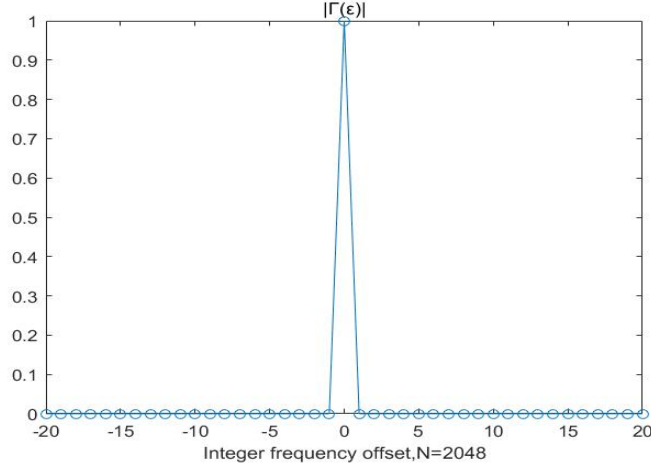


Figure 5.4: $|\Gamma(\varepsilon)|$

Therefore, in order to reduce the influence of IFO, we use differential cross-correlation as:

$$\begin{aligned}
 J_2(s) &= \frac{1}{M} \sum_{n=0}^{N-1} \{r(n+s)r^*(n+s-A)S^*(n)S(n-A)\} \\
 &= e^{j\frac{2\pi\varepsilon}{N}} \sum_{l=1}^{L_{channel}} \sum_{m=1}^{L_{channel}} c_l c_m^* \frac{1}{N} \sum_{n=0}^{N-1} \{S(n+s-\tau_l)S^*(n+s-A-\tau_l)S^*(n)S^*(n-A)\}
 \end{aligned} \tag{5.7}$$

We denote $q(n) = S(n)S^*(n-A)$ which has a good auto-correlation property. The coherent part in terms of $q(n)$ in $J_2(s)$ is:

$$J_{2a}(s) = e^{j\frac{2\pi\varepsilon}{N}} |c_i|^2 \tag{5.8}$$

which will have $L_{channel}$ peaks at $s = \tau_i (i = 0, 1, \dots, L_{channel})$. In order to achieve a good auto-correlation property of $q(n)$, we choose A as 50. Based on the coarse header detection, the search window here can be limited to $-\frac{L_b}{2} \leq s \leq \frac{L_b}{2}$, where L_b is the length of the beacon's guard interval.

To further improve the accuracy, we could multiply the auto-correlation function of the beacon symbol with the differential cross-correlation function to reduce the unwanted minor peaks [38]. The spectrum mode whose reference beacon produces a peak will be chosen as the estimated spectrum mode.

One example is shown in Figure 5.5, where the actual spectrum mode is 9. Figure 5.5(a) where the reference beacon from mode 9 is used, has a peak value compared with that in Figure 5.5(b). Moreover, besides the major peak, there are two minor peaks in Figure 5.5(a), this is when the received signals are cross-correlated with one of the two identical parts in the reference beacon instead of the whole reference beacon.

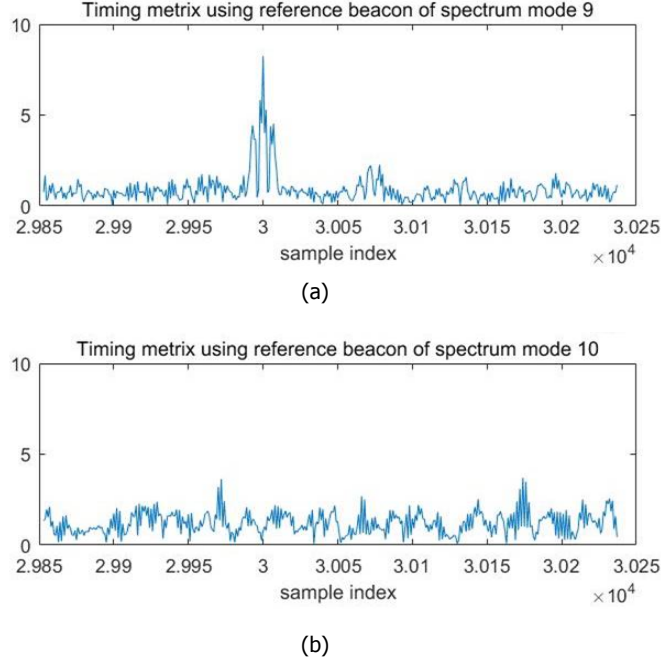


Figure 5.5: Differential cross-correlation

5.3. Carrier frequency offset correction

The carrier frequency offset is caused by the frequency mismatch in the transmitter and the receiver oscillators, and the Doppler effect as the receiver is moving. It is divided into an integer frequency offset (IFO) which causes the index shift as well as phase shift in the received frequency-domain signals, and a fractional frequency offset (FFO) which introduces attenuation in magnitude, phase shift, and ICI. The FFO is corrected by the Moose algorithm [39] after the robust mode detection, which remains unchanged with Yun's design [2]. The IFO is corrected after the spectrum mode detection when the unique reference beacon signal is determined.

5.3.1. Proposed algorithm

The newly proposed IFO detection method is based on the idea of the periodogram, which has a lower computational complexity and is more robustness against adjacent channel interferences compared as in Yun's design [2].

By multiplying the received beacon signal with the reference beacon, we have:

$$\begin{aligned}
 P_x(d) &= r(d, \varepsilon)S^*(d) \\
 &= \left\{ \sum_{m=0}^{L_{channel}-1} h(m)S(d-m)e^{\frac{j2\pi\varepsilon d}{N}} + w(d) \right\} S^*(d) \\
 &= h(0)|S(d)|^2 e^{\frac{j2\pi\varepsilon d}{N}} + \sum_{m=1}^{L_{channel}-1} h(m)S(d-m)S^*(d)e^{\frac{j2\pi\varepsilon d}{N}} + w(d)S^*(d)
 \end{aligned} \tag{5.9}$$

where ε is the number of subcarriers shifted. The problem is equivalent to detect a signal with frequency $f_k = \varepsilon/N$ in a complex tone. To realize the frequency estimation, we apply the idea of a periodogram

[40] and the estimated IFO is as follows:

$$\hat{\varepsilon} = \frac{1}{2} \underset{\varepsilon}{\operatorname{argmax}} |I(\varepsilon)| \quad (5.10)$$

where

$$I(\varepsilon) = \sum_{d=0}^{N-1} P_x(d) e^{-\frac{j2\pi\varepsilon d}{N}} \quad (5.11)$$

which is similar to a DFT operation. The factor $\frac{1}{2}$ is used because in the time domain, the beacon body has two identical parts which means that in the frequency domain, only the odd subcarriers are filled with information while the even subcarriers are padded with zeros.

As we can see, the algorithm proposed has a wide detection range between $-N/2$ to $N/2$, and a low computational complexity. One example is shown in Figure 5.6, where there is an obvious peak showing the estimated IFO value.

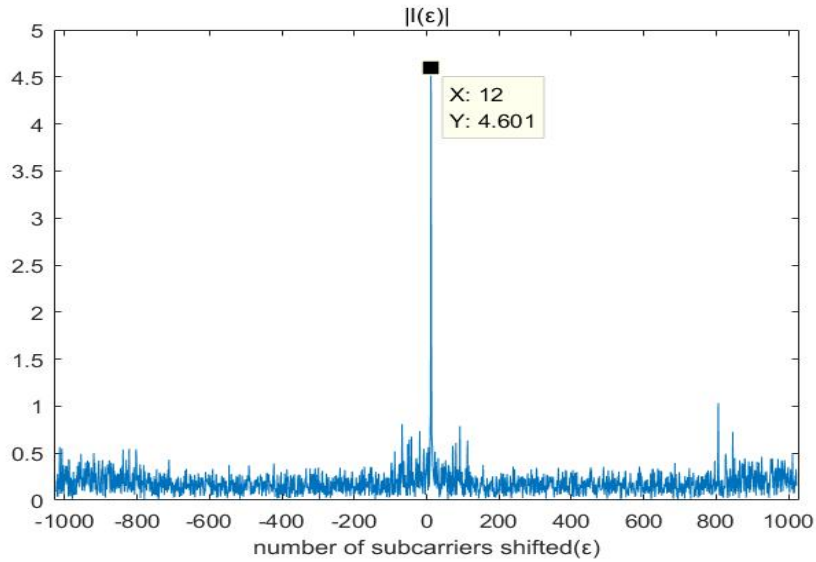


Figure 5.6: $|I(\varepsilon)|$, Tx mode 1, Spec mode 9

6

Adjacent-channel FM signal interference removal

This chapter explains the detailed design of the adjacent-channel FM signal removal block, the orange block in Figure 4.2, which is used to detect whether an adjacent-channel FM signal exists at a certain carrier frequency spacing from the host hybrid signal, and is above a certain power level, and to reduce its interference if necessary.

The impact of the adjacent-channel FM signal on the host-channel CDR signal depends on their power ratio and their carrier frequency spacing. As discussed in Section 3.2.2, if the carrier frequency spacing between the host and adjacent-channel signal is 200kHz, the two FM signals will overlap with each other, which will be avoided in designing the broadcasting network. If the spacing is equal to or more than 400kHz, the overlap between the adjacent-channel FM and host OFDM sub-carriers is limited. In this case, by a bandpass filter, we could remove the interfering signal. Only when the spacing is 300kHz and the overlapped power ratio of the adjacent-channel FM to the CDR digital is relatively high will cause a serious impact on the reception quality of the CDR digital signal. In the following of this section, we take the case of stereo FM broadcasting and CDR spectrum mode 9 (which is commonly used for the CDR test network in China) as an example.

The adjacent-channel FM removal block is composed of two main functional blocks, which is an energy detector and an FM removal, as illustrated in Figure 6.1.

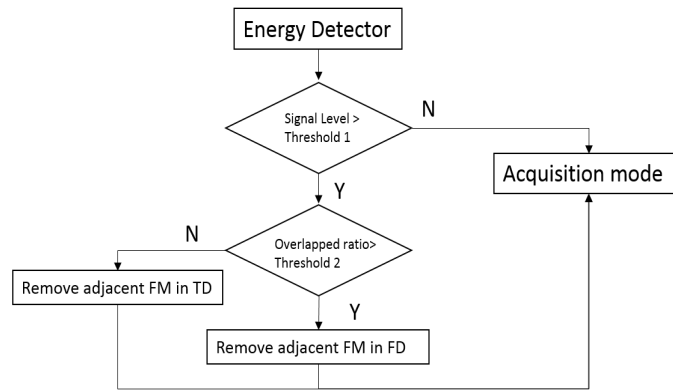


Figure 6.1: Adjacent-channel FM detector

The received signal first passes the energy detector, which is used to detect the existence of the FM signal whose carrier frequency is 300kHz from the host hybrid signal. If the adjacent-channel signal level is higher than a certain threshold, the receiver will enter the second step to estimate the power ratio of the host FM to the adjacent-channel FM signal. If the ratio is higher than a second threshold, the interfering FM signal will be filtered out by a frequency-domain method. Otherwise, the interfering signal will be removed by a time-domain method. After the adjacent-channel interfering signal is removed, the receiver will enter its acquisition mode.

The following section introduces the algorithms implemented in the energy detector and the adjacent FM removal block.

6.1. Energy Detector

The energy detector is used to detect whether an adjacent-channel FM signal exists at a carrier frequency spacing of 300kHz. And if it exists, the energy detector could further measure and estimate the power of this adjacent-channel signal. The main idea is to measure the power of subcarrier bins in the 200kHz-450kHz bandwidth. If it exceeds a threshold, the power of the FM signal located in the 150-200kHz frequency band, which is also the CDR's digital sideband, is predicted by a linear interpolation from the measured power.

As shown in Figure 6.6, the received signal is transformed from the time domain to the frequency domain by a 2048-point FFT using a rectangular window. By averaging the FFT bins for several time instances, the signal power in the 200kHz-450kHz band could be measured.

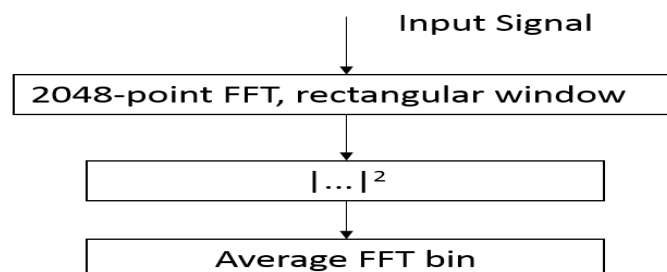


Figure 6.2: Energy detector

According to our simulation results, the spectrum of FM signal (in dB scale) can be interpreted as a triangle function, which is also mentioned in [16]. Based on the signal located at frequency 200-

300kHz, its slope and intercept can be computed by a linear interpolation, which is used to predict the power of the FM signal located in the 150-200kHz frequency band. One example is shown in Figure 6.3, where the green curve represents the estimation of the FM signal's PSD at 150-200kHz frequency band.

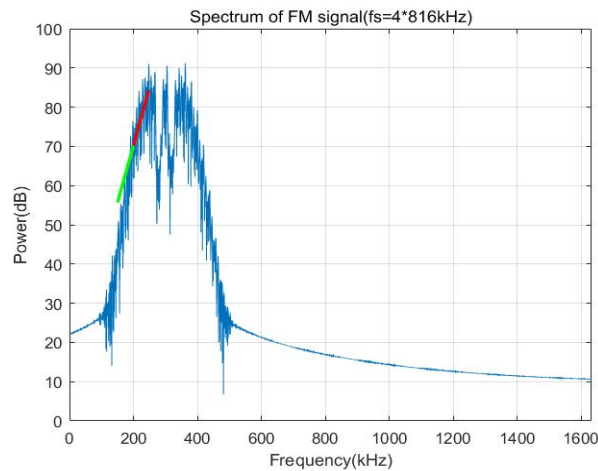


Figure 6.3: FM power linear interpolation

The accuracy of this prediction method is shown in Figure 6.4. The estimation error of the adjacent-channel FM's power are mainly from -2dB to +2dB.

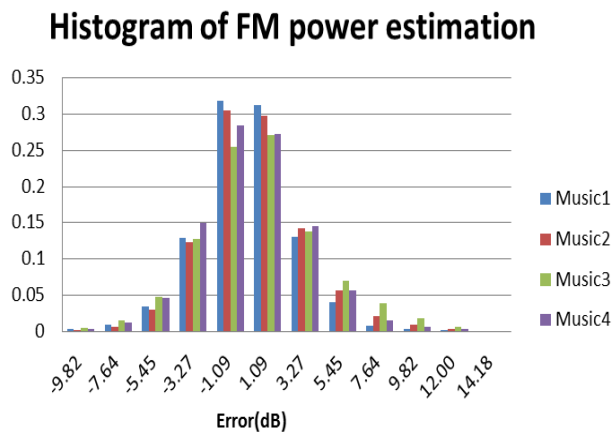


Figure 6.4: Histogram of FM power estimation

6.2. FM interference removal

To remove an FM signal interference, two methods are proposed in this section. The frequency-domain method works when the overlap power ratio of the digital to the FM signal in the digital sideband is higher. And the second method works when this ratio is within a certain range.

6.2.1. Frequency-domain (FD) method

In the FD method, as shown in Figure 6.5, the input signal is segmented and converted into the frequency domain. We only take the signals at the digital sidebands convert them back to the time

domain and used as the estimated digital signal for further processes.

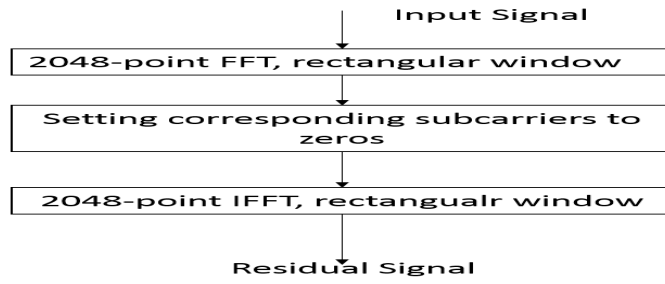


Figure 6.5: FD method

6.2.2. Time-domain (TD) method

The idea of this method is to first reconstruct the FM signal by estimating its amplitude and phase, and subtract it from the hybrid signal, where the residual signal is treated as the estimated digital signal. In the following section, we will explain how this algorithm works.

Assuming the received signal is:

$$r(t) = Ae^{j\theta(t)} + d(t) \quad (6.1)$$

where $Ae^{j\theta(t)}$ is the interfering FM signal, and $d(t)$ is the baseband digital signal. We assume $A \gg |d(t)|$ and A remains constant in one OFDM symbol time.

The estimated digital signal is expressed as:

$$\begin{aligned} \hat{d}(t) &= r(t) - \hat{A}e^{j\hat{\varphi}(t)} \\ &= (|r(t)| - \hat{A}) \frac{r(t)}{|r(t)|} \end{aligned} \quad (6.2)$$

where $\hat{\varphi}(t)$ and \hat{A} are the estimated phase and amplitude of the FM signal respectively.

The phase of the FM signal is assumed to be the same as the hybrid signal $r(t)$ based on the assumption that $A \gg |d(t)|$, and expressed as follows:

$$\begin{aligned} e^{j\hat{\varphi}(t)} &= \frac{r(t)}{|r(t)|} \\ &= e^{j\theta(t)} + \frac{d(t)}{A} \end{aligned} \quad (6.3)$$

The amplitude of the hybrid signal can be obtained by either taking the absolute value of the hybrid signal $r(t)$ directly or multiplying $r(t)$ with its conjugate phase information ($e^{-j\hat{\varphi}(t)}$). By substituting $e^{-j\hat{\varphi}(t)}$ from Equation 6.3, the amplitude of $r(t)$ is as follows:

$$\begin{aligned} |r(t)| &= \frac{r(t)r^*(t)}{|r(t)|} = r(t)e^{-j\hat{\varphi}(t)} \\ &= \left(e^{j\theta(t)} + \frac{d(t)}{A}\right)(Ae^{-j\theta(t)} + d^*(t)) \\ &= A + d^*(t)e^{j\theta(t)} + d(t)e^{-j\theta(t)} + \frac{|d(t)|^2}{A} \\ &\approx d^*(t)e^{j\theta(t)} + d(t)e^{-j\theta(t)} + A \end{aligned} \quad (6.4)$$

The first two components in Equation 6.4 are spread over the whole bandwidth, while the last item is condensed to a very narrow range around the zero frequency. The spectrum of Equation 6.4 is shown in Figure 6.6, where the blue curve represents the term $d^*(t)e^{j\theta(t)} + d(t)e^{-j\theta(t)}$ and the red curve represents the term A . The components that are around the zero frequency are considered to mainly come from the FM signal.

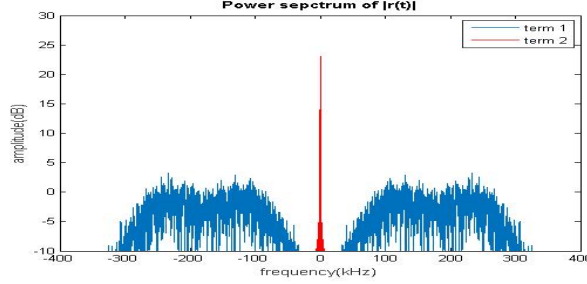


Figure 6.6: Spectrum of $|r(t)|$

By doing an FFT on $|r(t)|$ and taking the components around the center frequency, we get an estimation of \hat{A} . By substituting $|r(t)|$ with Equation 6.4 and $e^{j\hat{\phi}(t)}$ with Equation 6.3, Equation 6.2 becomes:

$$\begin{aligned}
 \hat{d}(t) &= (|r(t)| - \hat{A})e^{j\hat{\phi}(t)} \\
 &= (A - \hat{A} + d^*(t)e^{j\theta(t)} + d(t)e^{-j\theta(t)})(e^{j\theta(t)} + \frac{d(t)}{A}) \\
 &= (\Delta + d^*(t)e^{j\theta(t)} + d(t)e^{-j\theta(t)})(e^{j\theta(t)} + \frac{d(t)}{A}) \quad (6.5) \\
 &= \Delta \cdot e^{j\theta(t)} + \frac{d(t) \cdot \Delta}{A} + \frac{|d(t)|^2}{A}e^{j\theta(t)} + d(t) + \frac{|d(t)|^2}{A}e^{-j\theta(t)} + d^*(t)e^{2j\theta(t)} \\
 &\approx d^*(t)e^{2j\theta(t)} + d(t) + \delta
 \end{aligned}$$

where $\delta = \Delta \cdot e^{j\theta(t)} + \frac{d(t) \cdot \Delta}{A}$ is the estimation error introduced by Δ , which is the difference between the actual and estimated amplitude of FM signal.

The bandwidth of the first term on the right is twice as the second term, as is shown in Figure 6.7. Equation 6.5 gives an estimation of the digital signal despite of the phase noises that are introduced.

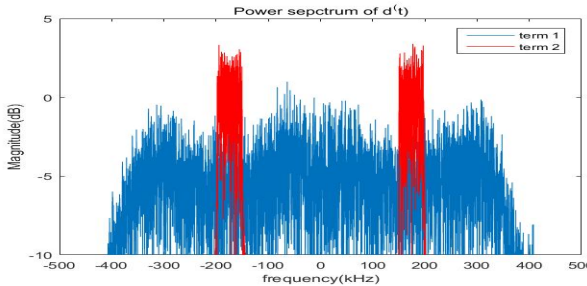


Figure 6.7: Spectrum of $\hat{d}(t)$

To conclude, the processes of the proposed algorithm are to get the phase of the input signal which is used as an estimation of FM signal's phase, to estimate the amplitude of the FM signal by doing an FFT on $|r(t)|$ and taking the components around the zero frequency, and to subtract the estimated FM

signal from the hybrid signal, as shown in Figure 6.8.

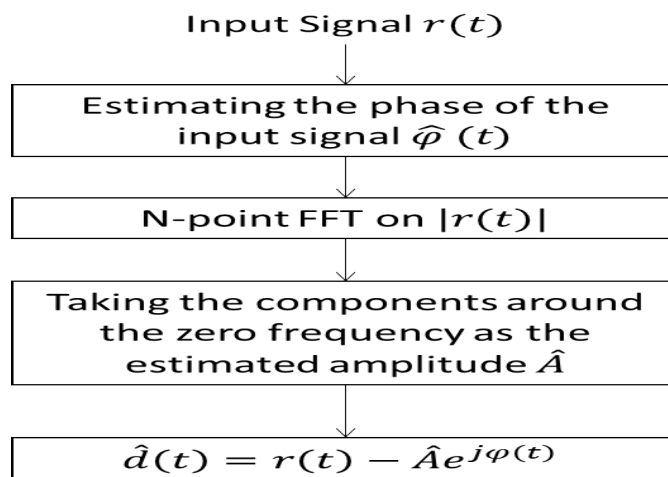


Figure 6.8: Time-domain method

7

Simulation results and performance analysis

This chapter provides simulation results and analyses of the acquisition and reception performance of the modified digital receiver with the existence of the co-channel and adjacent-channel FM interference. In the co-channel interference scenario, performance under multiple spectrum modes and constellation mapping schemes are tested. In the adjacent-channel interference scenario, the reception performances with different power ratios of the host FM to the adjacent-channel FM signal at a fixed carrier frequency spacing at 300kHz are tested using the algorithms discussed in Section 6.2.

The performances are tested under both the AWGN channel and the TU6 channel with a mobility speed of 200 km/h. The TU6 channel refers to a Typical Urban channel model with 6 paths. Its properties are shown in Table 7.1, including different delays, average path gains and power spectrum models for every path.

Table 7.1: Properties of the TU6 channel

Path index	1	2	3	4	5	6
Delay (us)	0	0.2	0.6	1.6	2.4	5
Average path gain (dB)	-3	0	-2	-6	-8	-10
Power spectrum model	Jakes	Jakes	Bi-Gaussian	Bi-Gaussian	Bi-Gaussian	Bi-Gaussian

7.1. Acquisition performance

Our solutions have achieved very good mode detection and synchronization performance with the co-channel FM interference as shown in Table 7.2. In the table, the FM width means the estimation of the bandwidth reserved for the FM signal to be either 200kHz or 300kHz; the first process means the auto-correlation based only on a subframe beacon and the combined process means the algorithm computing the sum of periodic peaks of OFDM symbols is also used, as mentioned in Section 5.1.1; the Spectrum Mode is a combined estimation of FM width and the digital sidebands as discussed in Section 5.2; the SNR value means the ratio of digital signal power to white Gaussian noise power in dB scale.

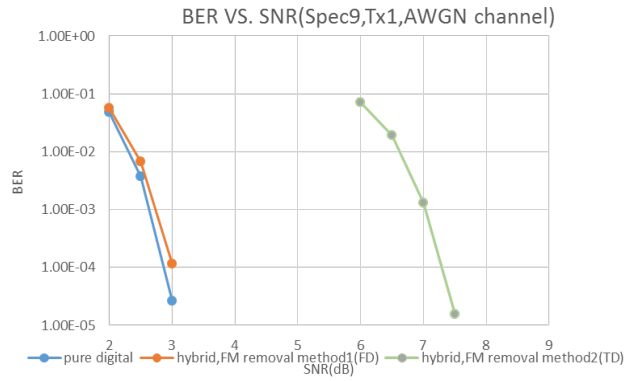
Table 7.2: Detection accuracy in acquisition mode

Transmission mode: 2; Spectrum mode: 9, AWGN Channel					
SNR(dB)	FM width (1st process)	Tx Mode (1st process)	FM width (Combined)	Tx Mode (Combined)	Spectrum Mode
1	92.5%	100%	100%	100%	88.75%
2	96.25%	100%	100%	100%	98.75%
3	96.25%	100%	100%	100%	100%
Transmission mode: 1;Spectrum mode: 9; TU6 Channel					
SNR(dB)	FM width (1st process)	Tx Mode (1st process)	FM width (Combined)	Tx Mode (Combined)	Spectrum Mode
6	76.56%	82.5%	98.44%	99.38%	99.38%
7	80.31%	85.62%	97.19%	98.75%	98.12%
8	85.62%	87.5%	98.12%	100%	99.38%
9	88.75%	88.75%	98.44%	100%	100%
Transmission mode: 1;Spectrum mode: 22; AWGN Channel					
SNR(dB)	FM width (1st process)	Tx Mode (1st process)	FM width (Combined)	Tx Mode (Combined)	Spectrum Mode
1	100%	100%	100%	100%	96.25%
2	100%	100%	100%	100%	97.5%
Transmission mode: 1;Spectrum mode: 22; TU6 Channel					
SNR(dB)	FM width (1st process)	Tx Mode (1st process)	FM width (Combined)	Tx Mode (Combined)	Spectrum Mode
4	87.5%	97.5%	93.75%	93.75%	85%
5	90%	95%	97.5%	98.75%	88.75%
6	91%	95%	98.75%	98.75%	93.75%

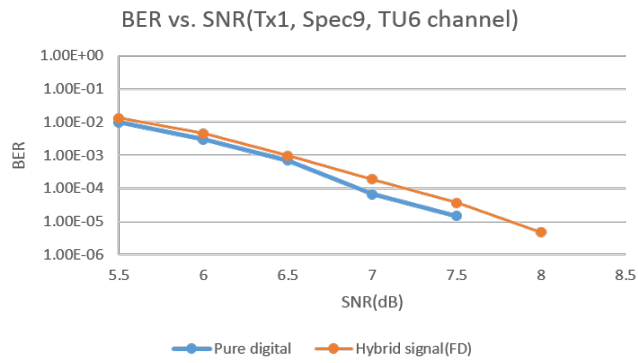
The detection accuracy of both the transmission and spectrum mode is more than 98% when the SNR is more than 2dB and 6dB under AWGN and in the TU6 channel environment respectively, and in the presence of a hybrid stereo FM broadcasting. The successful detection probability is higher than 95% under the AWGN channel even if the SNR is as low as 1dB with a mono FM interference. As noise power becomes smaller, the detection accuracy becomes higher. The second process outperforms the first process in both FM width and the transmission mode detection. Moreover, a second-round of detection could be employed to increase the accuracy, if the CRC of the decoded SI is wrong after the first detection round. To take the second simulation settings in Table 7.2 as an example, the failure probability after the first detection round is as low as 2% for both spectrum and transmission mode detection. Therefore, we expect the mode detection over two consecutive subframes should be successful in most cases.

7.2. The impact of co-channel FM on the reception performance

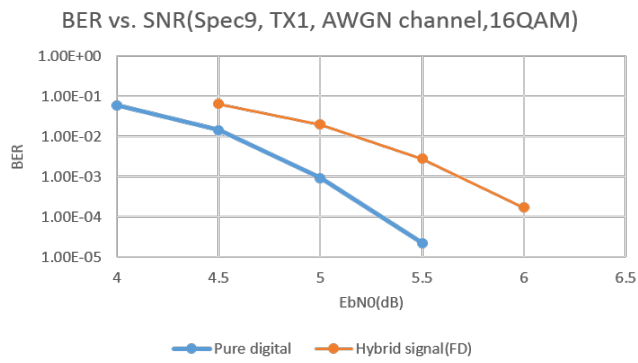
Figure 7.1 shows the receiver's performance in the presence of the co-channel FM signal with the configurations of the digital signal in Table 7.3. The blue curves represent the performance of pure digital signals without FM and the red and green curves for that of hybrid signals using different FM removal methods. The perceptual audio quality is acceptable when the BER is between 10^{-3} and 10^{-4} .



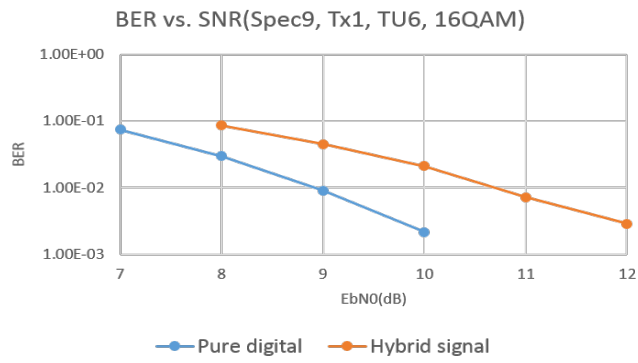
(a)



(b)



(c)



(d)

Figure 7.1: Performance under the existence of co-channel FM

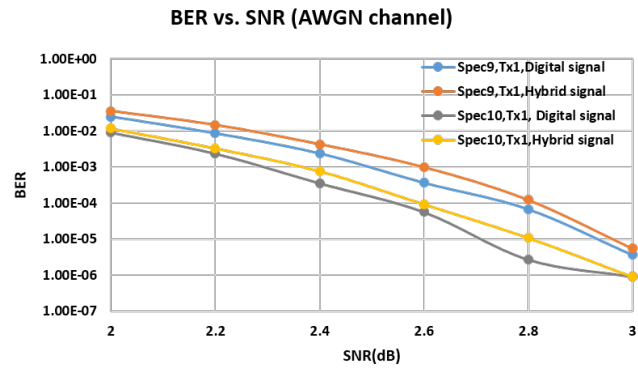
Table 7.3: Configurations used to derive simulation results in Figure 7.1

Tx Mode	Spec Mode	MSDS Modulation	SDIS Modulation	LDPC Coderate	LDPC iterations	Permutation Mode
1	9	QPSK/16QAM	QPSK	1/2	10	1

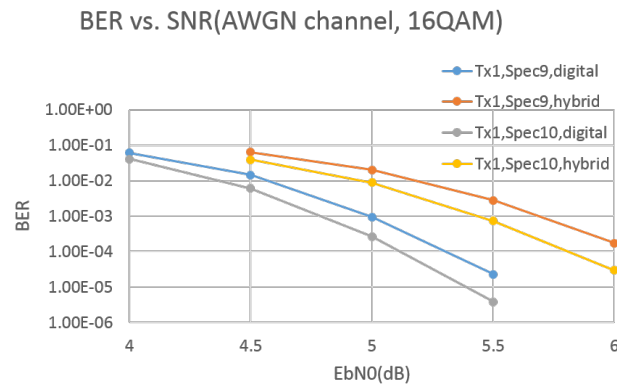
The digital signal reception performance suffers very little with co-channel FM interference by using the frequency-domain removal method mentioned in Section 6.2.1. Compared with the pure-digital-signal case, the SNR value degradation is less than 0.2dB to reach the same BER performance under both AWGN and TU6 channels for a QPSK modulation scheme. However, by changing the existing floating-point FFT operation to a fixed-point one, further degradation may be introduced due to saturation. By using the time-domain removal method, the SNR value is about 4dB higher to reach the same BER, which is a significant performance drop. Therefore, to reduce co-channel FM interference, the frequency-domain removal method is recommended.

Using a higher order modulation scheme requires a higher SNR value and the co-channel FM impact is more serious than that using the lower modulation scheme. For instance, in Figure 7.1(c), a 16QAM modulation scheme requires a 3dB SNR increase compared with the QPSK case. This loss is reasonable because compared with the QPSK, the transmitted energy in the 16QAM modulation remains almost the same, but more bits are transmitted. In the meanwhile, an SNR increase between 0.7 and 1dB is observed when comparing the performance of the hybrid signal with the pure digital signal in Figure 7.1(c) and Figure 7.1(d). One possible reason is that a higher order modulation scheme is more sensitive to the noise introduced by the FM signals.

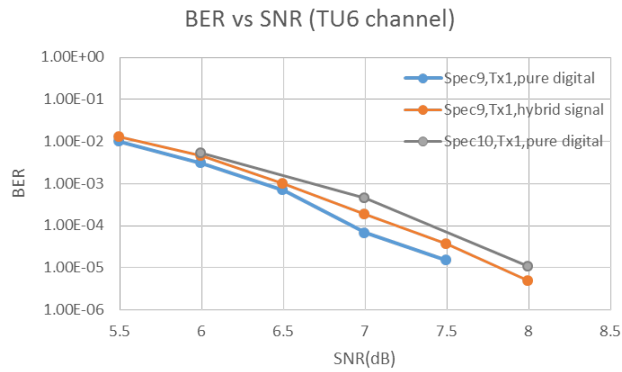
Figure 7.2 shows the performance of the modified receiver under different spectrum modes with the settings of the digital signal in Table 7.4.



(a)



(b)



(c)

Figure 7.2: Performance under different spectrum modes

Table 7.4: Configurations used to derive simulation results in Figure 7.2

Tx Mode	Spec Mode	MSDS Modulation	SDIS Modulation	LDPC Coderate	LDPC iterations	Permutation Mode
1	9/10	QPSK	QPSK	1/2	10	1

The performance of spectrum mode 10 is slightly better than mode 9 (a 0.2dB SNR gain for QPSK and a 0.5dB SNR gain for 16QAM) to reach a target BER of 10^{-3} under the AWGN channel. One possible reason is that there are pilots inserted in the junction of two sidebands under mode 10, which will give

a better continuity in channel interpolation. However, the performance of spectrum mode 10 is worse than that of mode 9 under the TU6 channel. One possible reason is that the transmission bandwidth of mode 10 (100kHz) is closer to the channel's coherent bandwidth (200kHz for TU6 channel), compared with that of mode 9 (50kHz). From Figure 7.3 we can see that when the transmission bandwidth approaches the coherent bandwidth, the channel is regarded to have a frequency selective fading. To cope with this fading effect, a better channel equalizer scheme is necessary.

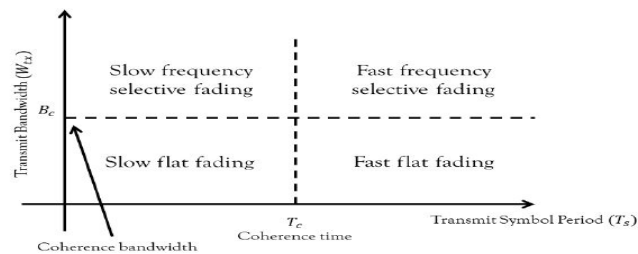
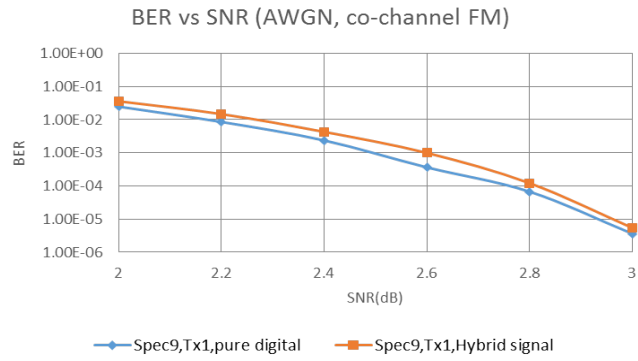


Figure 7.3: Multipath fading effects

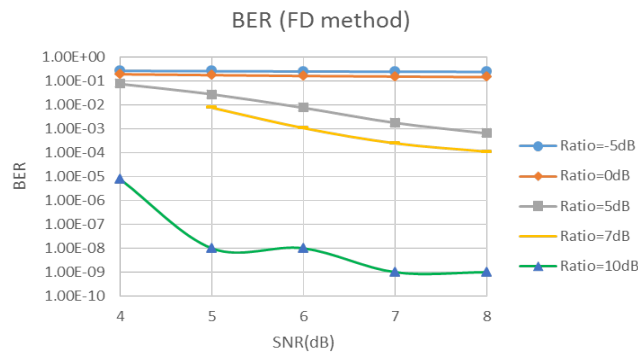
7.3. The impact of adjacent-channel FM on the reception performance

The receiver performances of the two adjacent-channel FM removal methods discussed in Section 6.2 are simulated and compared under both the AWGN and the TU6 channel. The carrier frequency spacing between the host and adjacent channel signals is set to be 300kHz.

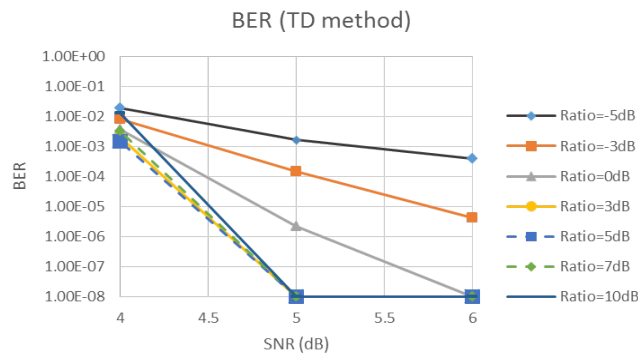
Figure 7.4 shows the performance under the AWGN channel, with the settings in Table 7.5. The ratio in the legend refers to the power ratio of the host FM to the adjacent-channel FM signal. The SNR means the power ratio of the digital signals to the AWGN noise, where the interference power from the FM signal is not included.



(a) Without adjacent-channel interference



(b) Frequency-domain method



(c) Time-domain method

Figure 7.4: Performance under the adjacent-channel FM interference (AWGN channel)

Table 7.5: Configurations used to derive simulation results in Figure 7.4

Tx Mode	Spec Mode	MSDS Modulation	SDIS Modulation	LDPC Coderate	LDPC iterations	Permutation Mode
1	9	QPSK	QPSK	1/2	10	1
Carrier frequency spacing:300kHz; Power ratio of host FM to adjacent FM at the receiver: -5 to 15dB; AWGN channel						

The interference brought by the adjacent-channel FM signal results in higher required SNR value compared with the co-channel interference case in the AWGN channel, as shown in Figure 7.4. If we can detect and select the better removal method in real time, we can control the performance degradation less than 3dB. The receiver works at an SNR value higher than 2.8dB with the interference

only from co-channel FM signal, as shown in Figure 7.4(a). For the FD removal method, as depicted in Figure 7.4(b), the receiver does not work when the power ratio is around or below 0dB. There is an SNR loss between 3 to 4 dB when the power ratio is between 5dB to 7dB, compared with Figure 7.4(a). If the power ratio is higher than 10dB, which means the signal from the adjacent-channel station is much lower than the host station, the FD removal method has a very good decoding performance even at a lower SNR value (less than 4dB). The TD method outperforms the FD method within a certain power ratio range, as shown in Figure 7.4(c). Compared with Figure 7.4(a), either a 3 dB or 1.5 dB SNR increase is introduced by using the TD method to reach a BER at 10^{-3} when the power ratio is -5dB or 0dB. By using the FD method, the BER value is always higher than 10^{-2} in these two cases. When the power ratio is between 0dB and 7dB, the TD method introduces an SNR increase of about 1.5dB compared with Figure 7.4(a), while the SNR increase brought by the FD method is doubled. To conclude, the TD method has a better performance when the power ratio of the host to the adjacent-channel FM signal is less than 10dB. If the ratio exceeds 10dB, a FD method works better. In order to select the best removal method, the energy detector proposed in Section 6.1 is required.

From a network perspective, the introduction of the TD method enables the user to be able to hear the host digital station in a larger coverage range compared with the performance of a FD method. Following the example illustrated in Section 3.2.2, the FM coverage area of two identically-configured stations is 56km and they are 80km apart, as shown in Figure 7.5.

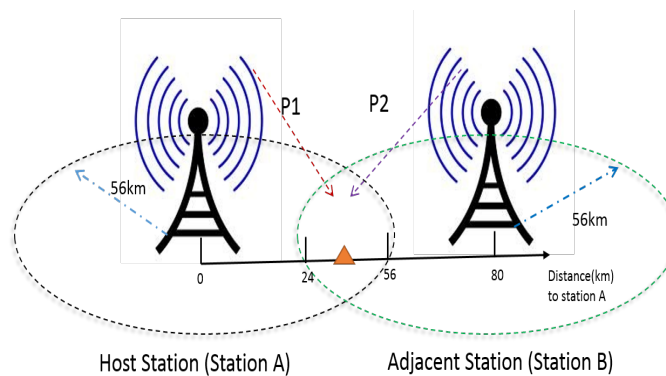


Figure 7.5: System model example

Based on the received power from station A and B in Table 7.6 (computation details in Appendix A), a relation between the power ratio and the user's distance to the host station is obtained, as shown in Figure 7.6.

Table 7.6: Power ratio of the system model example

Distance (km) to the host station	30	35	38	40
Received power from station A (dBkw)	89.31	83.57	80.17	77.87
Received power from station B (dBkw)	68.85	73.41	76.10	77.87
Power Ratio (dB)	20.46	10.16	4.07	0

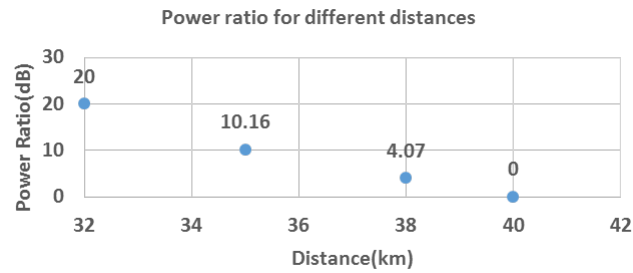
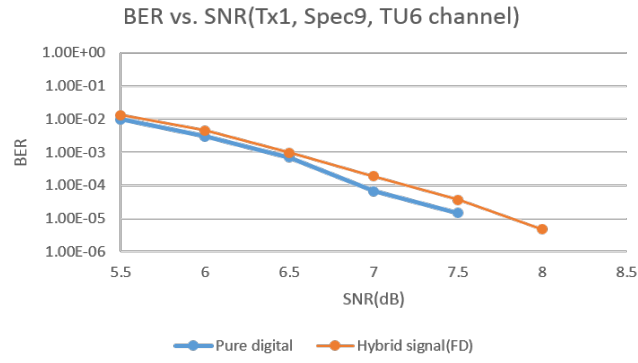


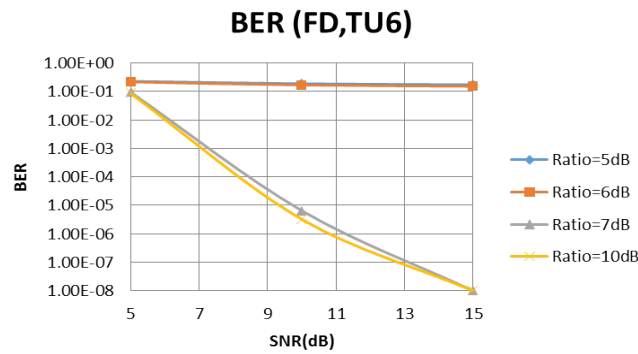
Figure 7.6: Relation between the power ratio and distances

Combining with the reception performance shown in Figure 7.4, we can see that if the user is at a range that is less than 35 km from the host station, the receiver has a better performance by using the FD removal method. If the user goes 3 km further away from the host station, the receiver needs to be switched to a TD removal method to reduce the impact of the interfering signal coming from station B. The reception quality of the signals from station A is acceptable when the user is in a range that is 35 km to 42 km to station A and the TD removal method is selected by the receiver. However, when the user is more than 42 km away from station A, it is impossible to hear from station A any more, because the BER is always as high as 10^{-1} .

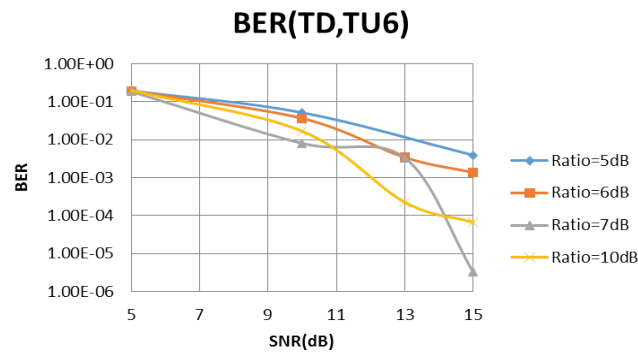
However, the reception is seriously impacted under the TU6 channel, as shown in Figure 7.7. Compared with the case in Figure 7.7(a), there is an SNR increase of at least 2.5dB. For example, when the power ratio is 7dB, the TD method and the FD method requires an SNR of 13.5 dB and 8.5 dB to reach a BER at 10^{-4} , while without the adjacent-channel interference, the required SNR value is about 7 dB.



(a) Without adjacent-channel interference



(b) Frequency-domain method



(c) Time-domain method

Figure 7.7: Performance under the adjacent-channel FM interference (TU6 channel)

One possible reason is that the estimated amplitude of the FM signal is inaccurate due to the multipath channel effect. We assume the received signal after a two-path fading channel is:

$$\begin{aligned}
 Y(t) &= a(t) \cdot r(t)e^{j\phi} + r(t) \\
 &= a(t)Ae^{j\theta(t)}e^{j\phi} + a(t)d(t)e^{j\phi} + Ae^{j\theta(t)} + d(t) \\
 &= \{a(t)e^{j\phi} + 1\}Ae^{j\theta(t)} + \{a(t)e^{j\phi} + 1\}d(t)
 \end{aligned} \tag{7.1}$$

where $a(t)$ and $e^{j\phi}$ represent the gain and delay of the channel path. The amplitude of $Y(t)$, as shown in Equation 7.2, is mainly composed of A and the component $a(t)A$, assuming $A \gg |d(t)|$, but it is not

a constant anymore.

$$|Y(t)| \approx \{a(t)e^{j\phi} + 1\}A \quad (7.2)$$

8

Conclusions and recommendations

8.1. Conclusions

In this project, the influences of the co-channel and adjacent-channel FM signals to the CDR digital signals are studied and analyzed. A transmitter chain with configurable CDR signals and FM signals is built and partly verified based on the test data from China. Design methods for mode detection and synchronization with the co-channel FM interference are established, and algorithms to detect and reduce adjacent-channel FM interference are proposed.

According to our simulation results, the mode detection accuracy for the hybrid signal is more than 98% when SNR is larger than 2 dB (AWGN channel) or 6 dB(Tu6 channel). The impact of co-channel FM signal on the digital signal is limited when using the modified receiver (less than 0.2dB loss for QPSK and 1dB loss for 16QAM to reach a target BER of 10^{-3}).

The FM interference from an adjacent channel 400 kHz away is less than the co-channel FM interference. The CDR network planning must avoid 200 kHz spacing case between adjacent channels. For the adjacent channel spacing of 300 kHz, if we can detect and select the better removal method by using an energy detector in real time, we can control the performance degradation less than 3dB under the AWGN channel. However, the performance under the TU6 channel experiences a more serious degradation under the impact of the adjacent-channel interference.

8.2. Recommendations for future work

Based on this project, several future works are recommended.

Firstly, a conversion from the floating-point to the fixed-point implementation is necessary to comply with the front-end processing.

Secondly, instead of filtering the FM signals by Fourier transformations, implementations with FIR filters are recommended to compare their performances.

Thirdly, more efforts can be made to improve the receiver's performance with the adjacent channel interference in mobile channel environments. For example, an iterative algorithm could be used to first subtract the FM signal, compensate the frequency offset computed from the residual signal to the

hybrid signal and estimate the FM signal for another round.

Fourthly, the performance of the receiver in a large-scale SFN needs be tested and analyzed.



Electric field Calculation

This section includes a translation of the technical specifications for FM broadcasting coverage networks in China [14] and an example calculated based on the specifications which is used in the report to illustrate the impact of adjacent-channel FM interference.

A.1. Service field strength

The service field strength, denoted as $E(50, 50)$, refers to the radio wave field strengths received directly by the public which exceeded during 50% of the time and 50% of the places. The service field strength is computed as follows:

$$E(50, 50) = P_e + E_1(50, 50) + G_r - F(\Delta h) \quad (\text{A.1})$$

where:

- P_e is the effective radiated power.
- $E_1(50, 50)$ is the normalized service field strength with $P_e = 1\text{W}$ and exceeded during 50% of the time.
- G_r is the receiving antenna gain plus the gain caused by different height of the receiving antenna.
- $F(\Delta h)$ is the attenuation correction factor.

The following part gives a more detailed introduction on how these parameters are computed.

A.1.1. P_e

The effective radiated power may be computed as follows:

$$P_e = P + G_t - L \quad (\text{A.2})$$

where P is the nominal output power of the transmitter, G_t is the gain of the transmission antenna and L is the feed line loss.

A.1.2. $E_1(50, 50)$

The normalized service field strength $E_1(50, T)$ is related to the effective height of the transmitter antenna (h_1), the distance apart from the transmitting station (d) and the percentage of time (T). Figure A.1 and A.2 show the normalized service field strength that exceeded 50% and 10% of the time respectively.

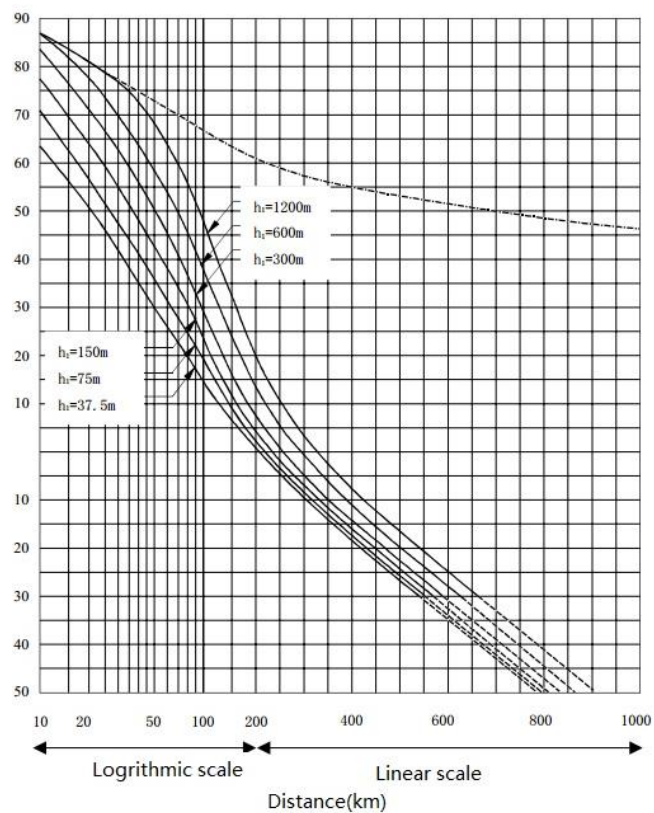


Figure A.1: Field strength ($\text{dB}\mu\text{V}/\text{m}$) for 1kW e.r.p.(50% of the time)

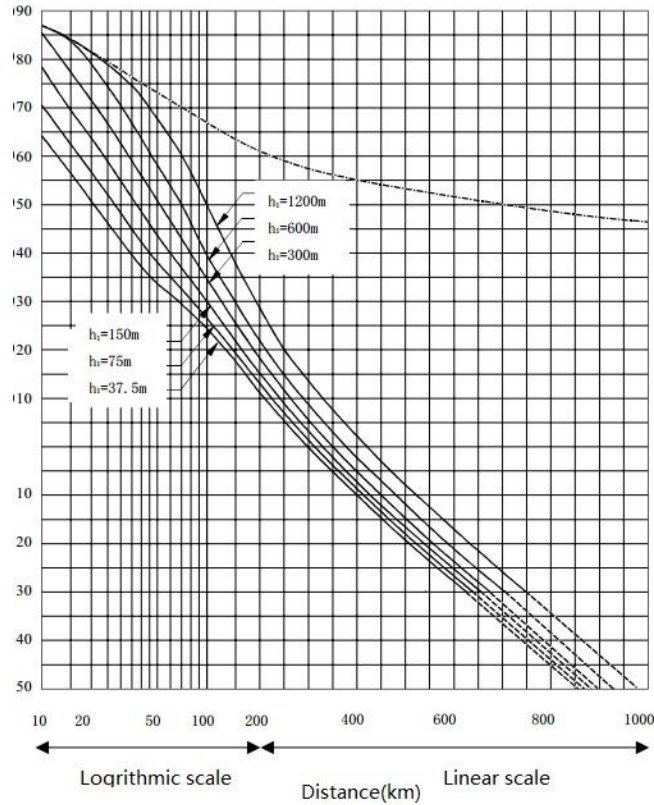


Figure A.2: Field strength ($dB\mu V/m$) for 1kW e.r.p.(10% of the time)

Several remarks when computing the normalized service field strength are as follows:

- Figure A.1 and A.2 are data obtained when the effective height of the receiving antenna is 10m, the degree of terrain irregularity is 50m and applicable in the VHF band.
- When the effective height h_1 is less than 10m, using the field strength value of $h_1 = 10m$.
- When the effective height h_1 is larger than 1200m, let:

$$dc = 70 + 4.1\sqrt{h_1(m)} \tag{A.3}$$

If the distance $d \geq dc$, the normalized service field strength is computed as:

$$E(h_1, d) = E(300, d + 70 - 4.1\sqrt{h_1}) \tag{A.4}$$

If the distance $d < dc$, the normalized service field strength is computed as:

$$E(h_1, d) = \begin{cases} E(1200, d) + E(300, 140) - E(1200, dc) & \text{if } 100 \leq d < dc(km) \\ E(1200, d) + \frac{d-20}{80}[E(300, 140) - E(1200, dc)] & \text{if } 20 < d < 100(km) \\ E(1200, d) & \text{if } d \leq 20(km) \end{cases} \tag{A.5}$$

where $E(h_1, d)$ means the service field with the effective height $h_1(m)$ and distance $d(km)$.

- A linear interpolation is used to compute the normalized service field for other distances (d) and

effective heights (h_1) which is not shown in Figure A.1 and A.2.

A.1.3. G_r

G_r is composed of the receiving antenna gain and the gain caused by the effective height of the antenna ($h_2(m)$), which can be computed as follows:

$$\text{Height gain(dB)} = \frac{c}{6} \cdot 20 \log_{10}(h_2/10) \quad (\text{A.6})$$

Typical c values are shown in Table A.1.

Table A.1: Typical height gain factors c

Zone	Value(dB)
Rural	4
Subrural	5
Urban	6

A.1.4. Correction factor

The attenuation correction factor is related to the degree of the terrain irregularity. Figure A.3 and Table A.2 shows the relation, where F_1 and F_2 are used for $d = 50\text{km} \sim 100\text{km}$ and $d \geq 200\text{km}$ respectively.

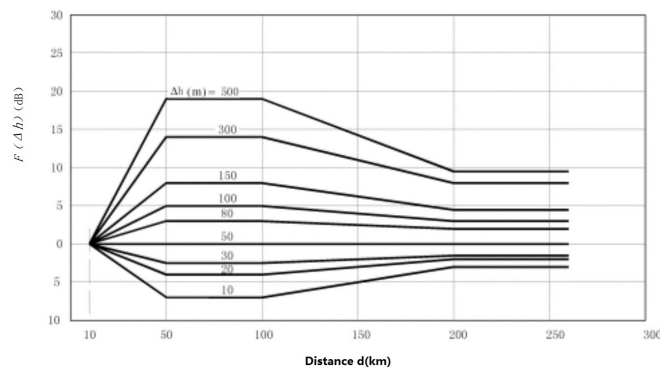


Figure A.3: Attenuation correction factor for different degrees of the terrain irregularity

Table A.2: Attenuation correction factor for different degrees of the terrain irregularity

Δh	F_1	F_2
10	-7.0	-3.4
20	-4.4	-2.4
30	-2.6	-1.5
40	-1.3	-0.7
50	0	0
60	0.7	0.6
70	1.9	1.1
80	2.6	1.5
90	3.5	2.0
100	4.3	2.4
150	7.6	3.9
200	10.0	5.2
300	13.9	7.0
400	16.9	8.2
500	18.9	9.1

Typical Δh values for different terrain types are shown in Table A.3 [41]. For an average terrain, Δh is 90m.

Table A.3: Typical Δh values

	$\Delta h(m)$
Flat or smooth water	0
Plains	30
Hills	90
Mountains	200
Rugged mountains	50

A.2. Interference field strength

The interfering field strength refers to the field strength received from the unwanted transmitter, and may be computed as:

$$E(50, T) = P_e + E_1(50, T) + G_r - F(\Delta h) \quad (\text{A.7})$$

A.2.1. $E_1(50, T)$

As we can see, when computing the interfering field strength, $E_1(50, 50)$ in Equation A.1 is replaced by $E_1(50, T)$. Different T values represent different interference type ($T = 10\%$ for tropospheric interference and $T = 50\%$ for steady interference). In order to determine the type of interference, nuisance field strength is used and computed as follows:

$$E_n = E_1(50, T) + A \quad (\text{A.8})$$

where A is the R.F. protection ratio, defined as the minimal difference between the service field strength and the interfering strength required at the input of the receivers for acceptable reception quality. The R.F. protection ratio is related to the carrier frequency spacing between the host and interfering stations, and typical values are shown in Table A.4.

Table A.4: R.F. protection ratio

Carrier freq spacing(kHz)	R.F. protection ratio(dB)	
	Steady interference	Tropospheric interference
0	45	37
100	33	25
200	7	7
300	-7	-7
400	20	-20

By computing $E_{ns}(50, 50)$ and $E_{nt}(50, 10)$ for steady and tropospheric interferences based on Equation A.8 and taking $\max(E_{ns}, E_{nt})$, we can determine the interference type.

A.3. Coverage area of a station

The coverage area of a station is related to its nominal usable field strength, which is the minimal field strength required under the influence of interference from industrial and domestic equipment. Typical nominal usable field strengths are shown in Table A.5. The range that satisfies the nominal usable field strength is the coverage of a station.

Table A.5: Typical nominal usable field strength values

Areas	$E_{nominal} dB\mu V/m$
Rural	54
Urban	66
Large cities	74

A.4. An example

This example shows how the coverage range of a station and the received power from the signal of a station is computed. In Section 3.2.2 and 7.3, this example is used to analyze the impact of adjacent-channel FM interference. We build a system model with two radio stations as shown in Figure A.4, which is explained in Section 3.2.2.

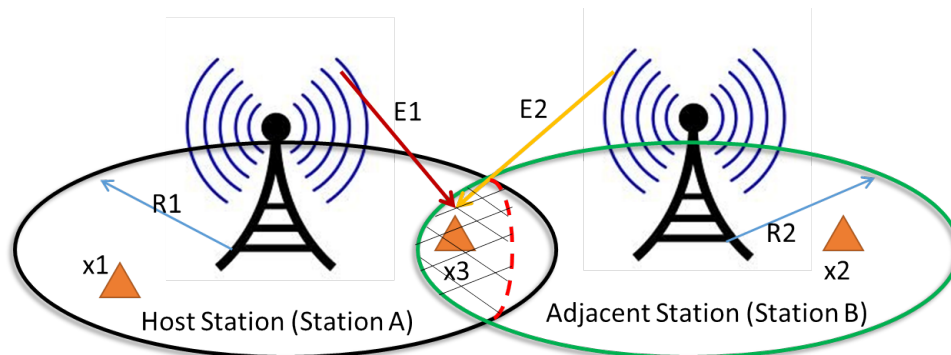


Figure A.4: System model for the adjacent FM interference

The settings of the two stations are assumed to be the same, which is shown in Table A.6.

Table A.6: Settings for station A and B

Path type	Urban
Transmitter nominal power P (dBkw)	40
Effective height of TX antenna h_1 (m)	150
TX antenna gain(dB) G_t	1.5
Degree of terrain irregularity(m) Δh	90
RX antenna height(m) h_2	2
Feedline loss(dB) L	0
RX antenna gain(dB) G_{r_1}	2.2

The service field strength of station A is:

$$E_A = P_e + E_1(50, 50) + G_r - F(\Delta h) \tag{A.9}$$

where:

- $P_e = 40 + 1.5 = 41.5dBkw$
- $G_r = G_{r_1} + \frac{c}{6} \cdot 20 \log_{10}(\frac{h_2}{10}) = 2.2 + 20 \log_{10}(\frac{2}{10}) = -11.7794dB$
- $F(\Delta h)$ is computed from Table A.2 by a linear interpolation.
- $E_1(50, 50)$ is computed from Figure A.1.

We build a demo in this project, as shown in Figure A.5, and plot the electric field strength in Matlab, as shown in Figure A.6.



Figure A.5: Demo for network planning

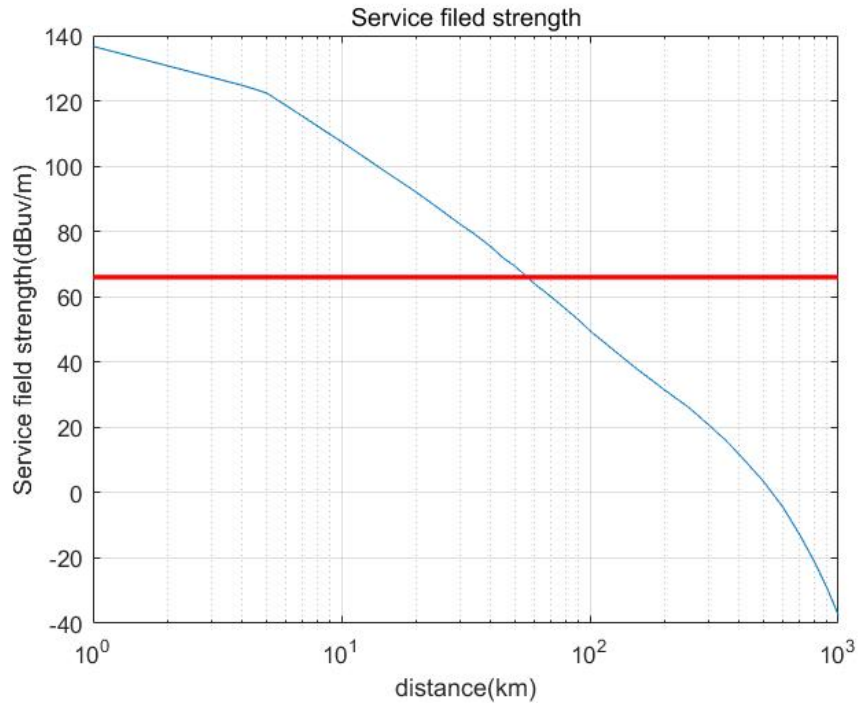


Figure A.6: Electric field strength of station A

Based on Table A.5, the coverage area of station A is 56km, to satisfy a minimal field strength of $66\text{dB}\mu\text{V}/\text{m}$.

Similarly, the interference field strength from station B can be computed based on Equation A.7. With the field strength E and the distance to the station d , the received power is computed as:

$$P_r = \frac{E^2 d^2}{30} \quad (\text{A.10})$$

We assume two stations are 80 km apart and their carrier frequency spacing is 300 kHz. The received power when the user is at different distances from the host station is shown in Figure A.7. The blue curve represents the field strength received by the user from station A, and the red represents that from station B. The green and black dotted lines are the maximal coverage of station A and B respectively. The pink dotted line indicates the maximal coverage area to satisfy the R.F. protection ratio if the user wants to listen to station A.

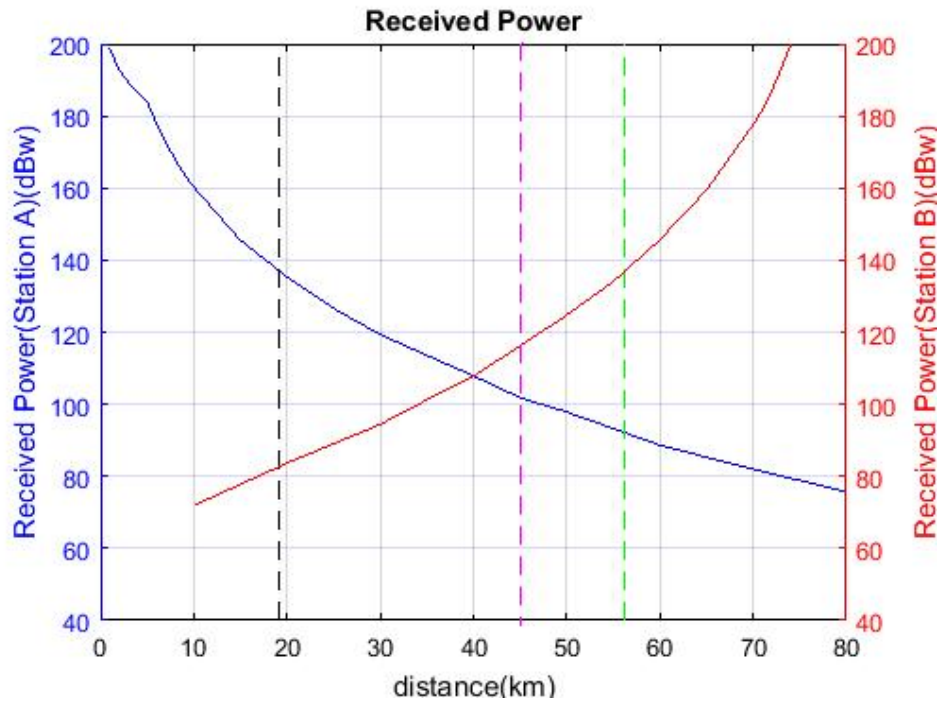


Figure A.7: Received power

For example, when the user is at a distance of 35 km from station A. From Figure A.7, the received power from station A and B is 96.61 dBkw and 66.07 dBkw respectively. The power ratio between the host and adjacent-channel FM signal is 30.53dB. Table A.7 lists several power ratio scenarios.

Table A.7: Power ratio of the system model example

Distance (km) to the host station	30	35	38	40
Received power from station A (dBkw)	89.31	83.57	80.17	77.87
Received power from station B (dBkw)	68.85	73.41	76.10	77.87
Power Ratio (dB)	20.46	10.16	4.07	0

B

Demo instructions

This section shows instructions on using the demo mentioned in Section 4.3.

B.1. Instructions

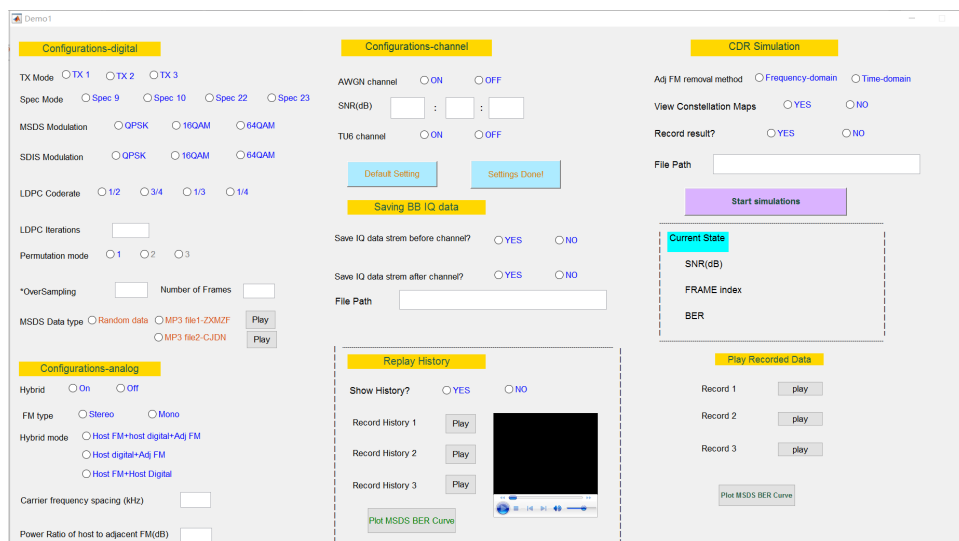


Figure B.1: Demo

The suggested steps in using the demo are as follows:

1. Transmission data configurations: Click 'Default Setting' or choose the settings by yourself and click 'Settings done!'
2. Receiving chain configurations:
 - Choose whether you want to view the constellation maps of LLRs before LDPC decoding

- Choose whether you want to record the decoded data. If yes, give the file path where the binary file will be stored. After the receiver finishes its process, you could hear the recorded data by clicking 'play' button in the section of "Recorded Data"
3. Running receivers' operating mode: Click 'Run Operation Mode', the receiver will start its process based on your configurations. After the receiver finishes its process, click 'MSDS BER curve' in the 'Recorded Data' section to see the BER vs. SNR curve
 4. Saving I/Q data: In the "Saving I/Q data" section, you can choose to save the I/Q data in a binary form both before and after channel environment.
 5. Showing history: When choosing 'Yes' for "Show history?", several decoded MSDS data that have been previous recorded based on your configurations will be available. Click 'Play' to hear their quality difference and 'MSDS BER Curve' in this section to see its BER curve.

B.2. Configurations

The screenshot shows a configuration window titled "Configurations-digital" with the following settings:

- TX Mode:** Radio buttons for TX 1, TX 2, and TX 3.
- Spec Mode:** Radio buttons for Spec 9, Spec 10, Spec 22, and Spec 23.
- MSDS Modulation:** Radio buttons for QPSK, 16QAM, and 64QAM.
- SDIS Modulation:** Radio buttons for QPSK, 16QAM, and 64QAM.
- LDPC Coderate:** Radio buttons for 1/2, 3/4, 1/3, and 1/4.
- LDPC Iterations:** A text input field.
- Permutation mode:** Radio buttons for 1, 2, and 3.
- *OverSampling:** A text input field.
- Number of Frames:** A text input field.
- MSDS Data:** Radio buttons for "Random data", "MP3 file1-ZXMZF", and "MP3 file2-CJDN". Each file selection has a "Play" button next to it.

- **System parameters of digital signal**
 - Transmission mode
 - Spectrum mode
 - Modulation scheme for MSDS and SDIS
 - LDPC code rate & number of iterations
 - Permutation mode (only mode 1 available)
- **Parameters of transmission data**
 - *oversample: sampling rate=816e3*oversample(Hz)
 - Number of Frames: 4 Frames=1 SuperFrame
 - MSDS Data: 3 streams of MSDS data available

Figure B.2: Digital signal configurations

- Analog signal setting:
 - Hybrid mode: on=adding FM signal, *over_sample should be greater than 4
 - FM type= Stereo for Spec.mode=9 and 10
 - FM type= Mono for Spec.mode=22 or 23
 - Hybrid mode: Adj FM are of all stereo type
- Channel setting:
 - SNR(dB)=min_value:step:max_value

Figure B.3: FM signal and channel environment configurations

B.3. Saving I/Q data

The real and imaginary part of the transmitted signal will be saved as I and Q data stream respectively in binary format under the assigned file path. The data are of 'double' precision and in a little-endian ordering. The stored I/Q data can be used for further test and simulations.

Figure B.4: Saving I/Q data

B.4. History

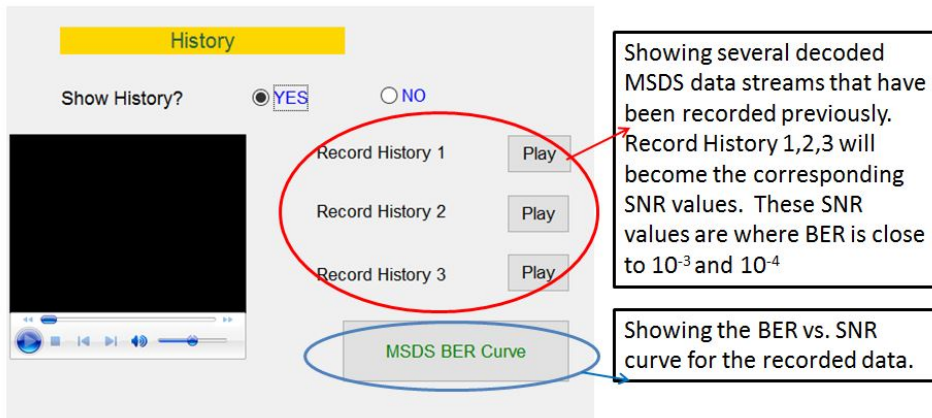


Figure B.5: History data

B.5. Operating mode

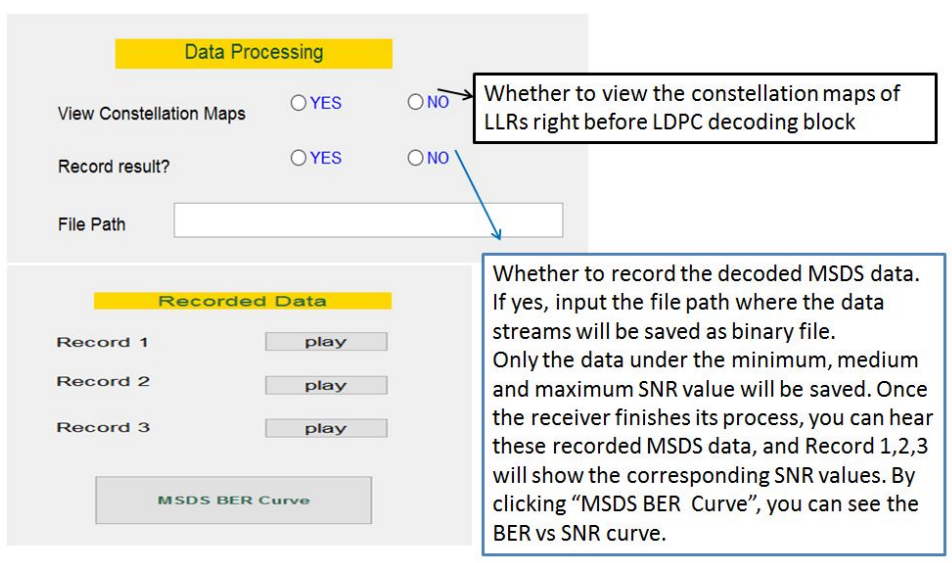
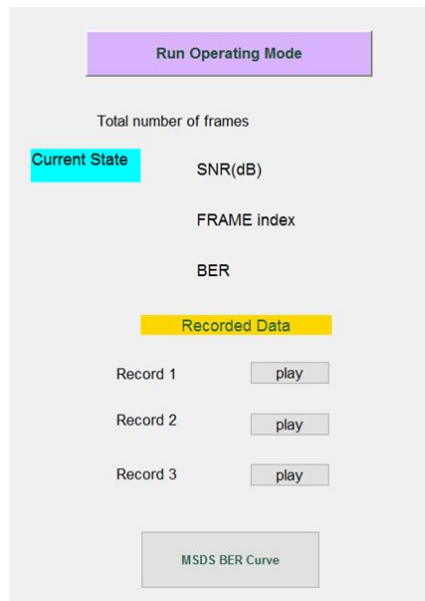


Figure B.6: Operating mode configuration



By clicking 'Run Operating Mode', the receiver starts its process. Total number of frames indicates the maximal number of frames that can be used from the input MSDS data. Current State shows the current SNR value, which frame is being processed, and its corresponding decoded BER value. After the receiver finishes its process, by clicking 'MSDS BER Curve', you will see the BER vs SNR curve.

Figure B.7: Real-time operating state

C

A list of abbreviations

AWGN	Additive white Gaussian nNoise
BER	Bit error rate
CCPLL	Cross-coupled phase-locked loop
CDR	Chinese Digital Radio
CFO	Carrier frequency offset
CPPC	Complementary punctured pair convolutional
CRC	Cyclic redundancy check
DAB	Digital Audio Broadcasting
DFE	Digital front-end
DFT	Discrete Fourier transformation
DRM	Digital Radio Mondiale
FD	Frequency-domain
FFO	Fractional frequency offset
FFT	Fast Fourier transformation
GUI	Graphical User Interface
IBAC	In-band Adjacent-channel
IBOC	In-band On-channel
ICI	Inter-channel interference

IFO	Integral frequency offset
ISI	Inter-symbol interference
ITU	International Telecommunication Union
LDPC	Low-density parity-check
LLR	Log-likelihood ratio
LO	Local oscillator
MSDS	Main service data symbol
OFDM	Orthogonal frequency-division multiplexing
PLL	Phase-locked loop
QAM	Quadrature Amplitude Modulation
QPSK	Quadrature Phase Shift Keying
RMD	Robustness Mode Detection
SCA	Subsidiary communications authorizations
SDIS	Service description information symbol
SDR	Software-defined radio
SFN	Single-frequency network
SGAPPRFT	State General Administration of Press, Publication, Radio, Film and Television
SI	Service Information
SIR	Signal-to-interference ratio
SNR	Signal-to-noise ratio
TD	Time-domain
TU6	6-tap Typical Urban

Bibliography

- [1] F. State Administration of Radio and Television, *Digital audio broadcasting in FM band—Part 1: Framing structure, channel coding and modulation for digital broadcasting channel*, Tech. Rep. GY/T268.1-2013 (State Administration of Radio, Film, and Television, 2013).
- [2] W. Yun, *SOFTWARE-DEFINED RADIO RECEIVER DESIGN AND DEVELOPMENT FOR CHINA DIGITAL RADIO (CDR)*, Master's thesis, Delft University of Technology, the Netherlands (2015).
- [3] Y. X. Wu Zhiyong and S. Guofang, *Coverage test of fm-cdr in beijing*, Radio and Television Information **1**, 37 (2014).
- [4] R. K. Tan, *Eureka-147 digital audio broadcasting*, Sound. Works magazine , 22 (1998).
- [5] D. P. Maxson, *The IBOC Handbook: Understanding HD Radio (TM) Technology* (CRC Press, 2007).
- [6] E. ETSI, *201 980: Digital radio mondiale (drm)*, System specification **2**, 2 (2005).
- [7] F. IBOC, *Transmission specification*, Ibiqity Digital Corp August (2001).
- [8] M.-K. Hu, *Visual pattern recognition by moment invariants*, Information Theory, IRE Transactions on **8**, 179 (1962).
- [9] G. Zhang, *Innovative technical solution for china s digital fm broadcast—brief introduction and comparison of cdradio and hd radio*, Electroacoustic Techniques **35**, 71 (2011).
- [10] F. State Administration of Radio and Television, *Technical specifications for FM sound broadcasting at VHF*, Tech. Rep. GY/T4311-2000 (State Administration of Radio, Film, and Television, 2000).
- [11] L. Der, *Frequency modulation tutorial*, Silicon Laboratories Inc (2008).
- [12] Wikipedia, *Fm broadcast band — wikipedia, the free encyclopedia*, (2015), [Online; accessed 23-May-2016].
- [13] *Technical specifications for coverage networks of FM sound broadcasting*, Tech. Rep. GY/T192 (State General Administration of Press, Publication, Radio, Film and Television, 2003).
- [14] F. State Administration of Radio and Television, *Technical specifications for coverage networks of FM sound broadcasting*, Standard (State Administration of Radio, Film, and Television, 2003).
- [15] SEMTECH, *Calculating radiated power and field strength for conducted power measurements*, (2007).
- [16] B. W. Kroeger and P. J. Peyla, *Compatibility of fm hybrid in-band on-channel (iboc) system for digital audio broadcasting*, Broadcasting, IEEE Transactions on **43**, 421 (1997).

- [17] S. Guofang, W. Tao, W. Ge, and W. Zhiyong, *Laboratory performance test for fm-band digital sound broadcasting systems (chinese)*, Radio and Television Information **1**, 44 (2014).
- [18] S. Guofang, W. Zhiyong, and Y. Fangzheng, *Research and coverage analysis on digital audio broadcasting in fm-band system (chinese)*, Program production and broadcast **38**, 73 (2014).
- [19] H. C. Papadopoulos and C.-E. Sunberg, *Simultaneous broadcasting of analog fm and digital audio signals by means of adaptive precanceling techniques*, Communications, IEEE Transactions on **46**, 1233 (1998).
- [20] B. Chen and C.-E. W. Sundberg, *Digital audio broadcasting in the fm band by means of contiguous band insertion and precanceling techniques*, Communications, IEEE Transactions on **48**, 1634 (2000).
- [21] J. N. Laneman and C.-E. W. Sundberg, *Soft selection combining for terrestrial digital audio broadcasting in the fm band*, Broadcasting, IEEE Transactions on **47**, 103 (2001).
- [22] B. Wang, *Iterative receiving technology research on digital-analog in band broadcasting system (Chinese)*, Ph.D. thesis, Beijing University of Post and Telecommunication (2013).
- [23] Y. Bar-Ness, F. Cassara, H. Schachter, and R. Difazio, *Cross-coupled phase-locked loop with closed loop amplitude control*, Communications, IEEE Transactions on **32**, 195 (1984).
- [24] J. Hamkins, *A joint viterbi algorithm to separate cochannel fm signals*, in *Acoustics, Speech and Signal Processing, 1998. Proceedings of the 1998 IEEE International Conference on*, Vol. 6 (IEEE, 1998) pp. 3297–3300.
- [25] J. N. Bradley, *Suppression of adjacent-channel and cochannel fm interference via extended kalman filtering*, in *Acoustics, Speech, and Signal Processing, 1992. ICASSP-92., 1992 IEEE International Conference on*, Vol. 4 (IEEE, 1992) pp. 693–696.
- [26] J. Hamkins, *An analytic technique to separate cochannel fm signals*, Communications, IEEE Transactions on **48**, 543 (2000).
- [27] B. Wang, J. Hou, P. Liu, and C. Xi, *Digital-analog in band separation using extended combined measurement kalman filter*, in *Wireless Personal Multimedia Communications (WPMC), 2012 15th International Symposium on* (IEEE, 2012) pp. 510–513.
- [28] W. Van Houtum and K. Kianush, *Communications with interference suppression*, (2015), uS Patent 20,150,358,040.
- [29] T. Sundresh, F. Cassara, and H. Schachter, *Maximum a posteriori estimator for suppression of interchannel interference in fm receivers*, IEEE Transactions on Communications **25**, 1480 (1977).
- [30] S.-J. Kim, K.-W. Park, K.-T. Lee, and H.-J. Choi, *Detection method for digital radio mondiale plus in hybrid broadcasting mode*, Consumer Electronics, IEEE Transactions on **59**, 9 (2013).
- [31] *HD Radio FM Transmission System Specifications*, Tech. Rep. SY-SSS-1026s (2008).
- [32] Y. Guan, *Research on frequency planning method of digital audio broadcasting in fm frequency band*, Radio and TV Broadcast Engineering , 127 (2013).

- [33] T. M. Schmidl and D. C. Cox, *Robust frequency and timing synchronization for ofdm*, Communications, IEEE Transactions on **45**, 1613 (1997).
- [34] A. Kurpiers and V. Fischer, *Open-source implementation of a digital radio mondiale (drm) receiver*, in *IEE conference publication* (London; Institution of Electrical Engineers; 1999, 2003) pp. 86–90.
- [35] C. Chen, B. Park, L. Wei, and H.-S. Oh, *Synchronization acquisition methods for drm systems*, in *Vehicular Technology Conference, 2006. VTC-2006 Fall. 2006 IEEE 64th* (IEEE, 2006) pp. 1–5.
- [36] L. Zeng, P. Zhang, S. Xu, and H. Yang, *Robustness mode detection algorithm in the drm system*, Broadcasting, IEEE Transactions on **54**, 792 (2008).
- [37] C.-R. Sheu and C.-C. Huang, *A differential sliding correlation scheme for symbol timing detection in time domain synchronous ofdm systems*, in *Vehicular Technology Conference, 2009. VTC Spring 2009. IEEE 69th* (IEEE, 2009) pp. 1–5.
- [38] A. B. Awoseyila, C. Kasparis, and B. G. Evans, *Robust time-domain timing and frequency synchronization for ofdm systems*, Consumer Electronics, IEEE Transactions on **55**, 391 (2009).
- [39] P. H. Moose, *A technique for orthogonal frequency division multiplexing frequency offset correction*, IEEE Transactions on communications **42**, 2908 (1994).
- [40] G. Ren, Y. Chang, H. Zhang, and H. Zhang, *Synchronization method based on a new constant envelop preamble for ofdm systems*, Broadcasting, IEEE Transactions on **51**, 139 (2005).
- [41] G. A. Hufford, A. G. Longley, W. A. Kissick, *et al.*, *A guide to the use of the ITS irregular terrain model in the area prediction mode* (US Department of Commerce, National Telecommunications and Information Administration, 1982).